Integration of Taste and Odor in Agranular Insular Cortex

Martin N. Vignovich

Submitted in partial fulfillment of the

requirements for the degree of

Doctor of Philosophy

under the Executive Committee

of the Graduate School of Arts and Sciences

COLUMBIA UNIVERSITY

2019

ABSTRACT

Integration of Taste and Odor in Agranular Insular Cortex

Martin N. Vignovich

Our perception of the world is limited by the senses we are endowed with. In the case of taste, its functional fidelity is so critical for our survival that we come into the world with innate preference for sweet and disgust for bitter. These stereotyped behaviors are hardwired at the lowest levels of taste processing and they support the view that taste serves as an arbiter of the chemical world, passing judgement before permitting ingestion. Yet our experience of foods is manifold. This complexity results from distinct contributions from the sights, sounds and smells of the foods we consume. Of these, odors are a co-equal component of flavor and the impairment of olfaction can disrupt enjoyment of eating and alter patterns of consumption. The goal of this thesis is to identify the neural basis of odor-taste perception and to characterize how neural activity is affected by odor-taste integration.

In contrast to the discrete and innate categorization performed by the taste system, the sense of smell enables discrimination of thousands of unique odor percepts which have no innate value. At the level of olfactory cortex, odor representations are randomly distributed and have been shown to be conditioned through association with other stimuli. The act of eating produces near simultaneous taste and odor transduction originating from the same source. Yet despite ultimately projecting to neighboring cortical regions, taste and odor pathways are anatomically segregated prior to reaching the cortex.

Using viral tracing strategies, we identified Agranular Insular cortex (AIc) as a putative site of odor-taste integration. We then used *in vivo* two-photon Ca^{2+} Imaging to characterize odor and taste responsive neurons and identify changes in population activity when these stimuli

were simultaneously presented. We next asked whether specific flavor experiences altered activity in AIc compared to naive animals. Finally, we developed a behavioral task to test whether silencing AIc disrupted perception of a flavor compound.

Contents

List of Figures

Chapter 1

Introduction and Background

In a landmark paper delineating the logic of sweet taste, the authors asked a simple question:

> "How many different receptors does it take to taste the sweet universe?"
>
> -*The Receptors for Mammalian Sweet and Umami Taste*

The answer is one. Or more specifically, one heteromeric receptor complex composed of two GPCRs. That the vast array of sweet molecules are all detected via a single receptor seems to flatten the world of sweets not to a plane but to a point. And yet we all have favorite flavors of equally sweet ice cream or jellybeans with the exact same nutritional content. It is the work of this thesis to understand how a point can become a universe.

A slime mold chemotaxing across a glucose gradient shows that intensity can provide a dimension of discrimination, but our perception of the chemical world is formed by multiple distinct senses whose interactions are poorly understood. Chemosensation is unique from other senses (vision, audition, and some types of somatosensation) in that the origin of the stimuli are so proximate as to enter the body and the variety of chemicals which can activate the sense is vast and disordered. While humans (and neuroscience) have evolved to give primacy to vision, chemosensation remains not merely as a vestigial set of senses, but as an integral realm of experience which ensures our survival and provides some of life's greatest pleasures.

Consumption of food can often feel like an automated action, performed so frequently and with such a controlled food supply that we try to entertain ourselves while we eat. Yet the act of eating is a process of testing our assumptions about the nutritional content and safety of foods. The disgust elicited by an unexpected hair in our mouth or the transcendence of an amazing meal can reify that moment in a way that shapes future behaviors.

Though the taste system provides an immediate report of the nutritional value (via receptor activation by sweets, salt, and proteins) and warnings of potential toxins (via bitter receptor activation), our memory of foods relies on unique multisensory experiences (comprised of the smell, taste, feel and temperature of the food among other qualities) being associated with an immediate evaluation of the food as well as post-ingestive effects. This thesis aspires to advance our understanding of where and how taste and odor, the two main senses that contribute to food identity, converge in the brain to form novel representations of the external world. We conducted experiments with the following aims and results:

1. Using our knowledge of taste and olfactory anatomy, we employ viral tracing strategies to identify a putative site of convergence – Agranular Insular cortex (AIc).
2. We employ functional calcium imaging to characterize the activity of cells in AIc in response to tastants, odorants, and mixtures. We then look at how these representations change in animals that have experience with a mixture.
3. We use a behavioral paradigm to ask whether silencing AIc impairs an animal's ability to discriminate a flavor mixture from its component odor and taste, demonstrating that performance on the task is selectively impaired in response to the flavor.

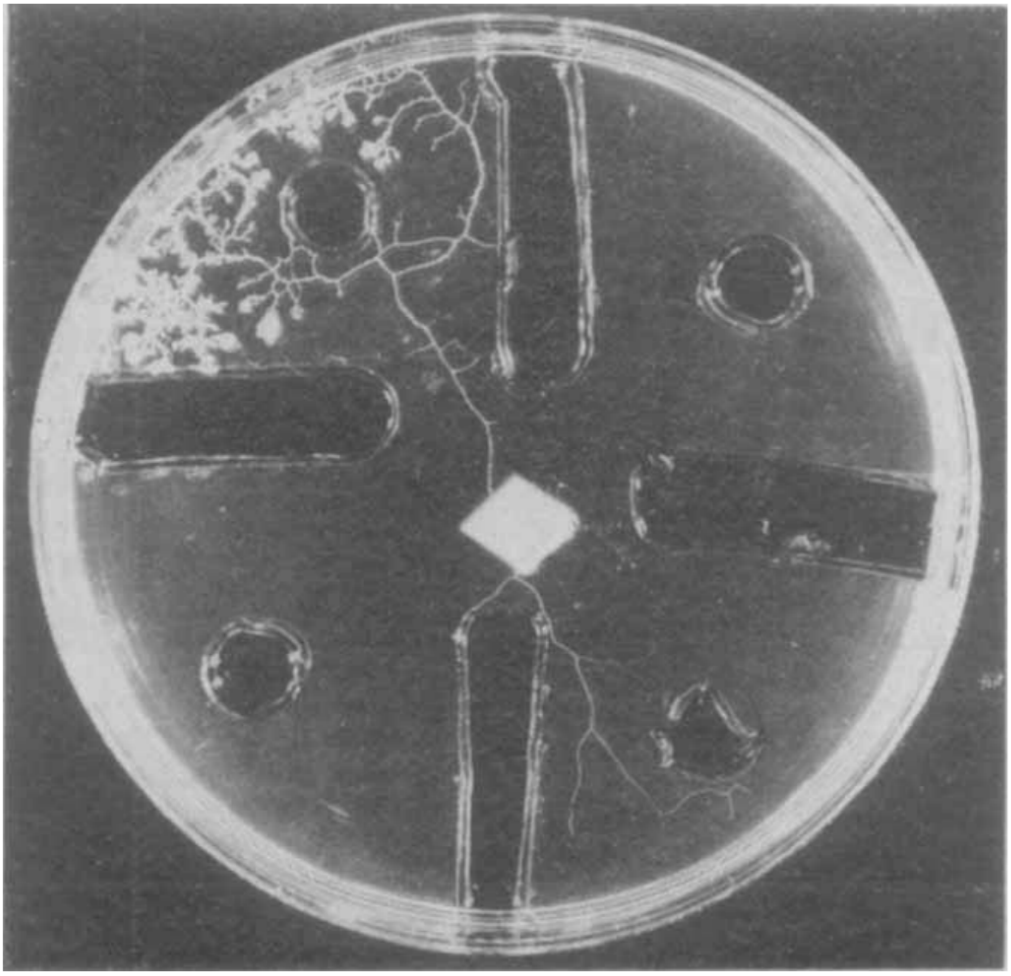

Fig 1.1: Chemotaxis in the Slime Mold Physarum polycephalum

Slime mold experience the environment as a linear gradient of attractive and repulsive substances, here moving towards a quadrant containing glucose (Chet et al., 1977).

Background

Taste

The sense of taste serves as an abettor of our basest instincts. Imbued with the ability to promote consumption of sweet tastes from nutritious substances while eliciting repulsion of bitter compounds which are often toxic, taste divides the world into pleasures necessary for survival and threats which imperil the taster. This segregation is innately hardwired from the tongue to the brain, allowing food to be evaluated and categorized before ingestion.

Our modern understanding of vertebrate taste began with the discovery of the receptors responsible for detection of chemicals present in the oral cavity (Adler et al., 2000; Chandrashekar et al., 2000; Damak, 2003; Matsunami et al., 2000). Transduction of chemical signals occurs in taste receptor cells (TRCs) which are bundled together in taste buds that pepper the oral epithelium of the tongue and palette of the mouth (Lindemann, 2001; Yarmolinsky et al., 2009). Each TRC expresses taste receptors that are sensitive to one of the five basic classes of taste quality: bitter, sweet, sour, salty, and umami. Thus, bitter cells express some subset of the taste receptor type 2 (T2R) repertoire and respond to a diverse array of potentially toxic molecules while sweet cells express the T1R2/T1R3 heteromeric receptor which recognizes both natural and artificial sweeteners (Adler et al., 2000; Damak, 2003; Nelson et al., 2001).

Unique TRC markers for each of the taste qualities have been identified and used to further probe the specificity and connectivity of these populations (Lee et al., 2017; Mueller et al., 2005; Zhang et al.; Zhao et al., 2003). These studies have revealed a labeled line organization on the tongue in which each TRC only expresses one class of receptor. Bitter, sweet and umami TRCs signal their activation via adenosine to nerve terminals of the facial nerve, whose cell bodies reside in the geniculate ganglion. Imaging studies of the geniculate

have demonstrated a broad concordance with the organization of separate taste classes seen on the tongue (Barretto et al., 2015).

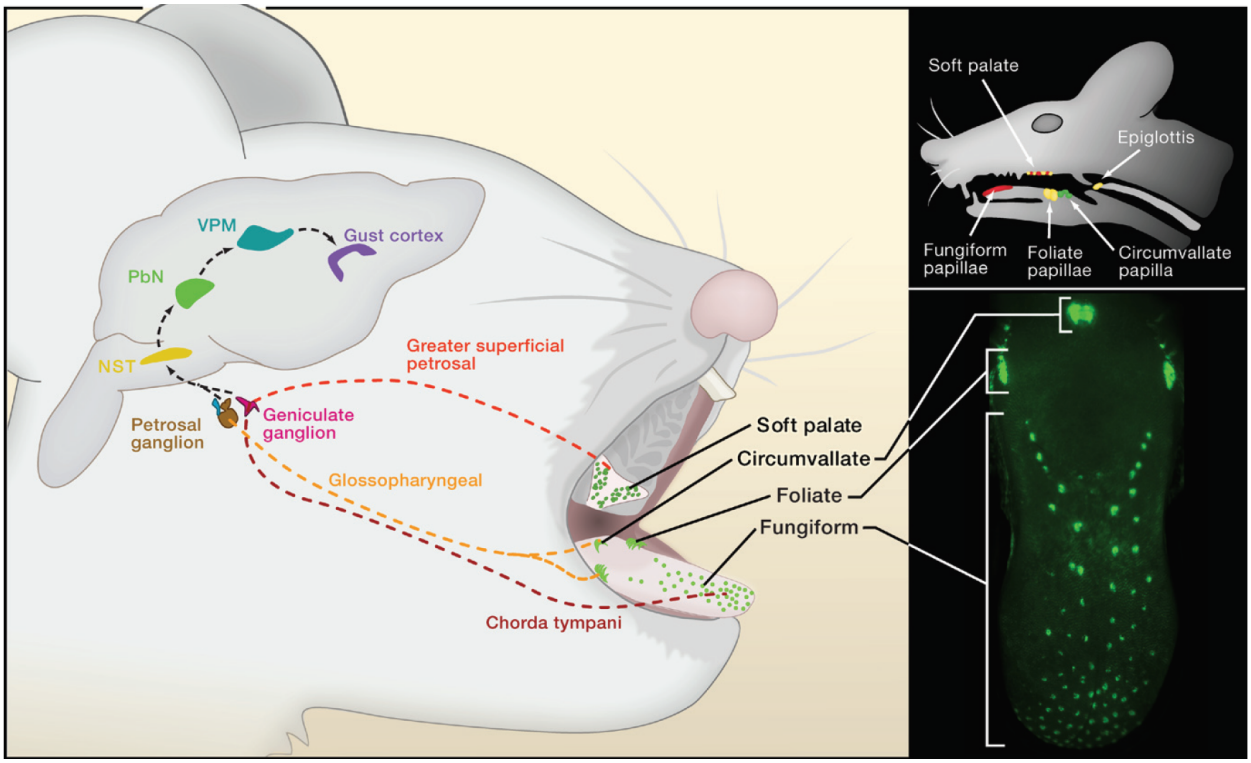

Fig 1.2: The anatomy of taste

Taste receptor cells are clustered in taste buds which are distributed across the tongue and palate (green dots, lower right, left). Taste buds are innervated by cranial nerves VII and IX. Taste information then travels through the brainstem (NST), the midbrain (PbN), thalamus (VPM) to Gustatory Cortex (Yarmolinsky et al., 2009).

Ganglion cells synapse onto cells in the nucleus of the solitary tract in the medulla which subsequently project to the parabrachial nucleus (a relay present in rodents but not primates) (Scott and Small, 2009), the ventral posteromedial nucleus of the thalamus, and then to the primary gustatory cortex (Norgren and Leonard, 1973; Saper and Loewy, 1980) (Fig 1.2). Gustatory cortex occupies a portion of the insular cortex, extending along the lateral surface of

the brain in mice with an anterior to posterior topographic organization whereby anterior neurons predominantly respond to sweet stimuli while posterior neurons largely respond to bitter (Accolla et al., 2007; Chen et al., 2011; Yamamoto, 1984). Furthermore, insular cortex is marked by a dorso-ventral laminar progression whereby the dorsal granular insula contains a thalamo-recipient layer 4 which becomes irregular and morphs into the agranular ventral insula which lies immediately adjacent to primary olfactory cortex (Gogolla, 2017).

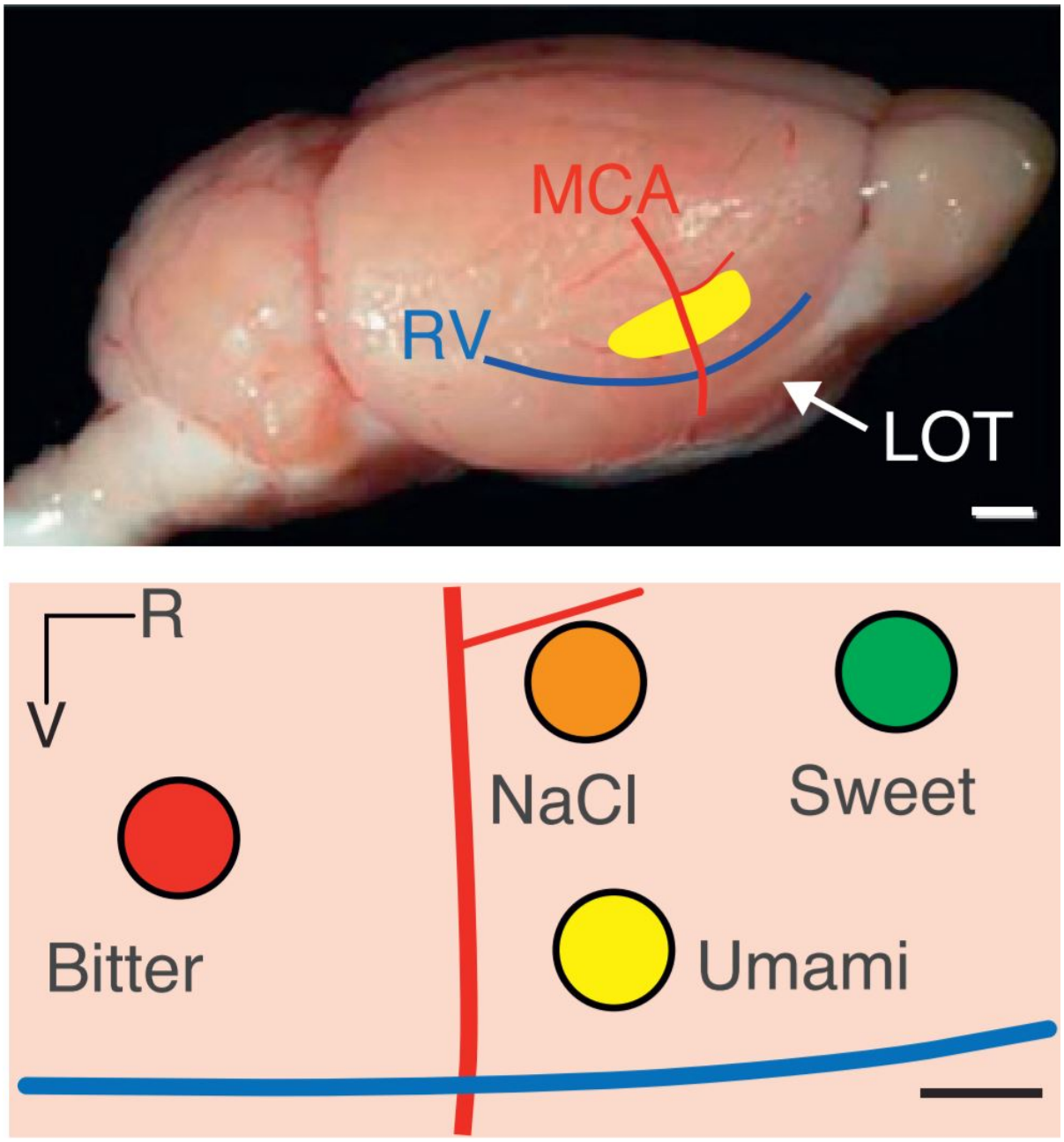

Fig 1.3 Taste Representations in Gustatory Cortex

Functional imaging provided evidence for a spatially segregated taste map whereby bitter cells are located caudally and sweet cells are located rostrally. These imaging locations were identified by vascular landmarks - the middle cerebral artery (MCA) and the rhinal vein (RV) (Chen et al., 2011).

The multiple stations of taste anatomy en route to the brain betrays the complexity of a sense which at first appears to serve as a binary discriminator of foods. At the most periphery, taste receptor cells activation is sufficient to elicit stereotypical aversive or appetitive behaviors to bitter or sweet stimuli. In animals with sweet TRCs which were engineered to express a receptor activated by a synthetic ligand, the animals avidly consumed that previously tasteless ligand (Zhao et al., 2003). Indeed, when a bitter receptor is expressed only in sweet cells, animals demonstrate a strong attraction to the normally bitter molecules that activate the receptor. Similar experiments in bitter taste receptor cells demonstrate that distinct populations of cells are hardwired to pathways which lead to innate stereotypical behaviors (Mueller et al., 2005). These behaviors can be characterized by consumption of a substance and facial reactions (such as "gaping, chin rubbing, and face washing" in response to bitter stimuli). In a testament to the hardwiring of these responses, decerebrate animals with all connections between the brainstem and the cerebrum retain the immediate appropriate responses to sweet and bitter substances (Grill and Norgren, 1978). Similarly, these "gustofacial" responses are present in anencephalic children (Steiner, 1973).

The evidence for hardwiring at the periphery and brainstem could be used to argue for a more expansive role in "higher" brain areas. If cortex is not required for these basic behaviors, is it still a slave to its inputs? Activation of cortical areas corresponding to sweet and bitter cortex has shown that animals respond to that activity as they would to those respective tastants (Peng et al., 2015; Wang et al., 2018). Furthermore, silencing of cortical taste areas using NBQX (an AMPA receptor antagonist) prevents animals from recognizing those tastants. Even in TRPM5 null mice which are incapable of tasting bitter or sweet, activation of bitter or sweet areas elicits aversion or attraction respectively. These experiments do not place a limit on what taste cortex is

capable of, but they establish that taste cortex is hardwired to connect taste inputs originating on the tongue to stereotyped behavioral outputs and that this behavior can be elicited through artificial activation.

Olfaction

In contrast to the innately valenced taste system with a few well segregated lines of information, olfaction provides a diverse distributed system which allows the multitude of detectable chemicals to be associated with salient objects and experiences.

The olfactory system is succinct in its organization, connecting olfactory receptor neurons in the nose to neurons in piriform cortex with just a few synapses. Transduction of odor molecules begins in olfactory sensory neurons (OSNs) in the nasal epithelium, each of which exclusively expresses one of the ~1000 odorant receptors (Buck and Axel, 1991; Godfrey et al., 2004; Zhang and Firestein, 2002). OSNs expressing the same receptor converge onto spatially defined glomeruli in the olfactory bulb, synapsing with mitral and tufted cells that project to piriform cortex (Ghosh et al., 2011; Sosulski et al., 2011). Notably, olfactory bulb does not significantly project to thalamus or any of the subcortical taste regions that project to primary gustatory cortex (Ongur, 2000; Shepherd, 2005).

Experiments tracing the outputs from a single glomerulus demonstrated that the spatial organization seen in the olfactory bulb is abandoned and each glomerulus projects diffusely throughout piriform cortex (Ghosh et al., 2011; Sosulski et al., 2011). In accordance with the anatomical studies, *in-vivo* 2-photon Ca^{2+} Imaging in piriform cortex has shown that odor-evoked responses are broadly distributed and partially overlapping (Stettler and Axel, 2009). This dispersed spatial organization differs from the clustered representations seen in taste cortex and reflects differences in the innate functions of these two systems. In contrast to taste, which constrains the ingestible chemical space into five qualities, the sense of smell allows for the discrimination of thousands (or potentially trillions) of odors in humans (Bushdid et al., 2014; Meister, 2015). And while taste is hardwired to trigger innate behaviors independent of

experience, the vast majority of odors have no meaning to a naïve animal and are afforded meaning only through experience and association (Choi et al., 2011; Gore et al., 2015).

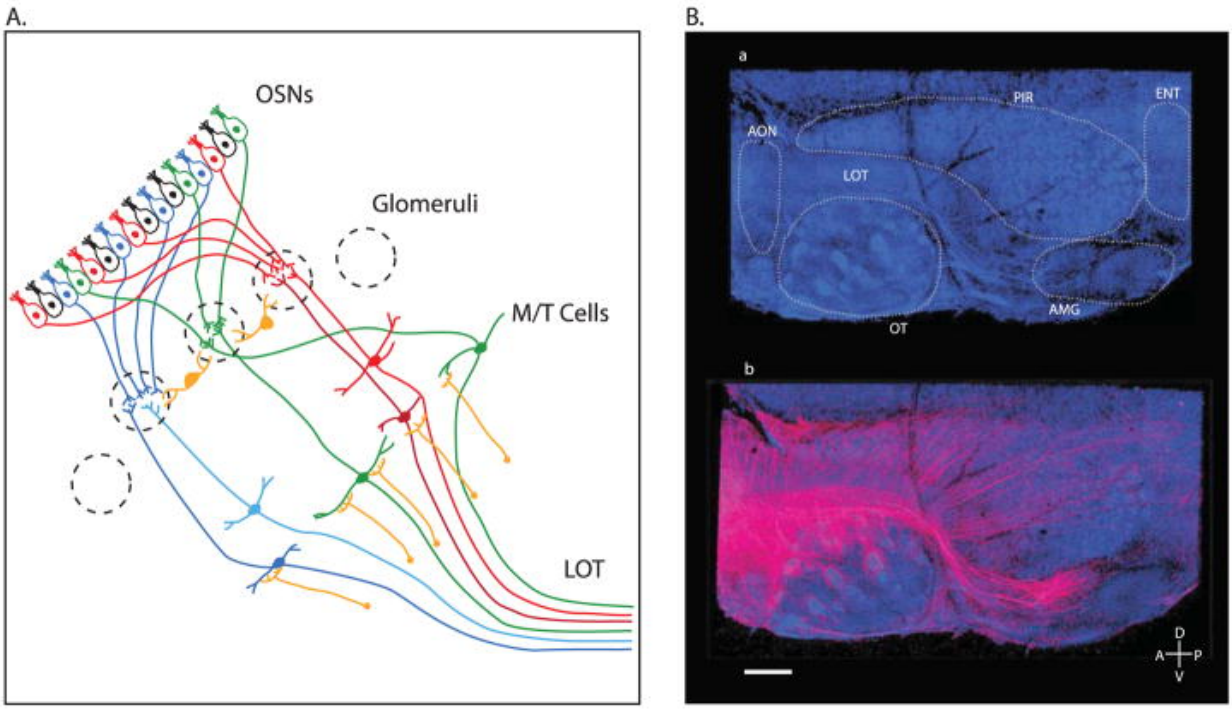

Fig 1.4: The Anatomy of Odor

Odor detection begins by binding of odors onto olfactory receptors in OSNs which project with spatial specificity to glomeruli in the olfactory bulb. Mitral and tufted (M/T) cells then project diffusely to olfactory cortical olfactory areas, including piriform cortex - the primary olfactory cortex (PIR). (Giessel and Datta, 2014)

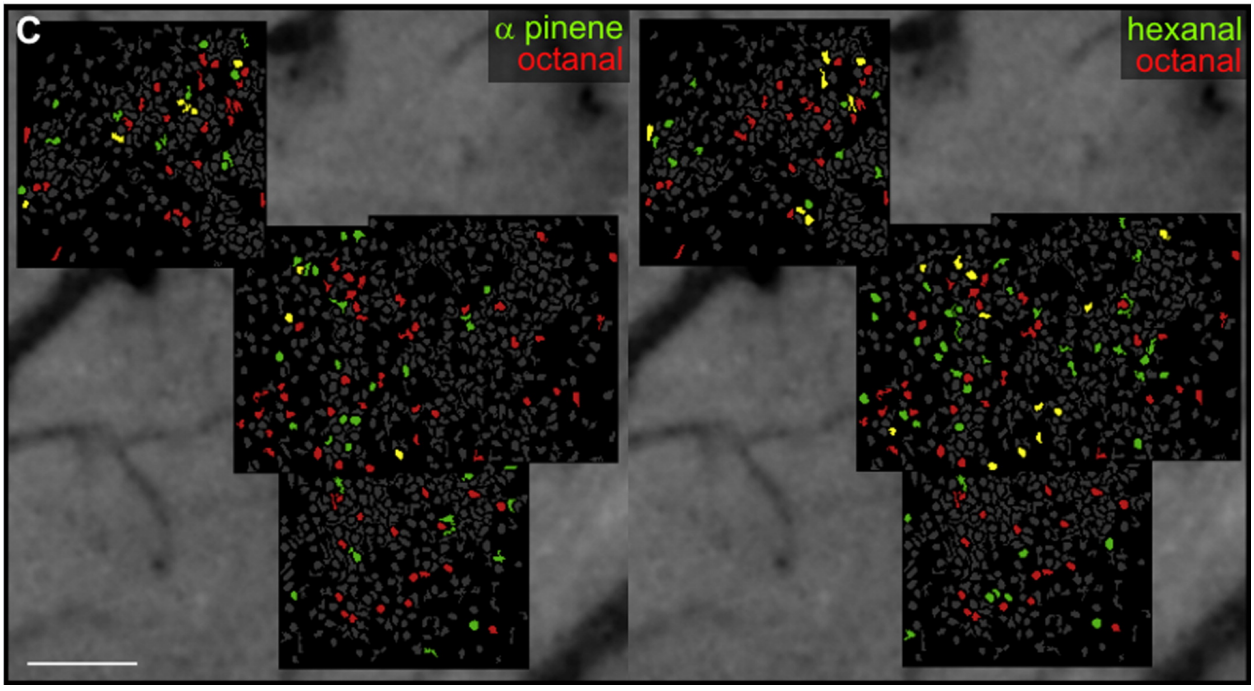

Fig 1.5. Odor is Represented in Overlapping Ensembles in Piriform Cortex

Classified responders to two different odors are overlaid with yellow cells responding to both odors. (Stettler and Axel, 2009)

Odor Taste Convergence in Agranular Insular Cortex

To identify prospective sites of odor taste integration, we asked where gustatory and olfactory cortical outputs converged. We unilaterally injected AAV(Synapsin-tdTomato) into posterior piriform cortex and AAV (Synapsin-GFP) into anterior gustatory cortex and looked for areas of overlap. The primary recipient of overlapping input from both regions was the Agranular Insular cortex (AIc) (Fig 1.6A).

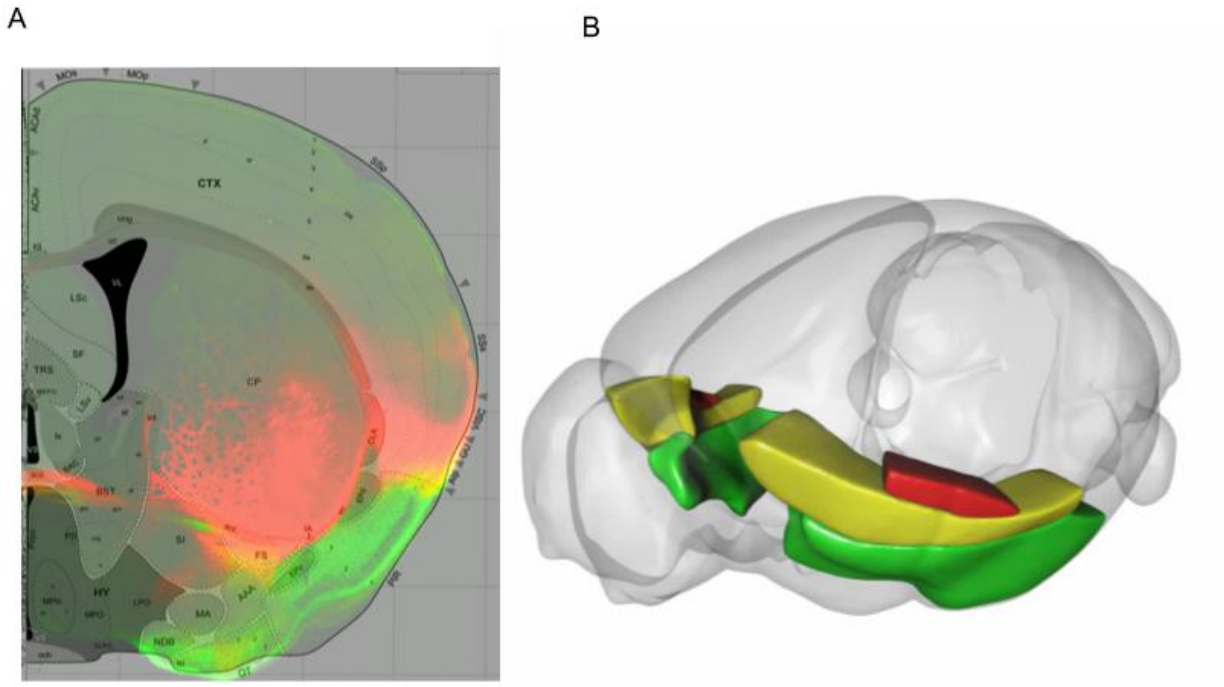

Fig 1.6: Taste and Odor Cortices Converge in Agranular Insular Cortex

A) Viral tracing showed the primary site of converge to be Agranular Insular Cortex. **B)** Agranular Insular Cortex (yellow) is located between primary gustatory (red) and olfactory(green) areas. (Allen Institute)

Agranular insular cortex is a five-layer cortical region (lacking the thalamo-recipient layer 4) located adjacent to primary gustatory and olfactory cortices (Fig 1.6B). In rats, two tracing studies have suggested evidence for AIc as a site of odor-taste integration. The first focused on outputs from piriform cortex using biotinylated dextran amine to reconstruct the morphology of two individual neurons. They found that the dorsal branches of the axonal arbor terminated in layer ⅔ of agranular cortex with projections extending several mm along the extent of AIc adjacent to taste cortex (Johnson et al., 2000a).

The second study used small volumes of biocytin injected with iontophoresis along the dorsal ventral axis of insular cortex. They found that only AIc received inputs from granular taste and piriform cortex. This led them to suggest that "...agranular insular cortex appears to be a multimodal sensory convergence zone for the insular and piriform cortices…"(Shi and Cassell, 1998a). Subsequent brain wide tracing studies have continued to report AIc as a distinct anatomical target of convergence (Zingg et al., 2014). These tracing results demonstrate convergence of fibers but if AIc is the primary site of odor taste integration, we would expect to find evidence of those fibers converging onto single cells.

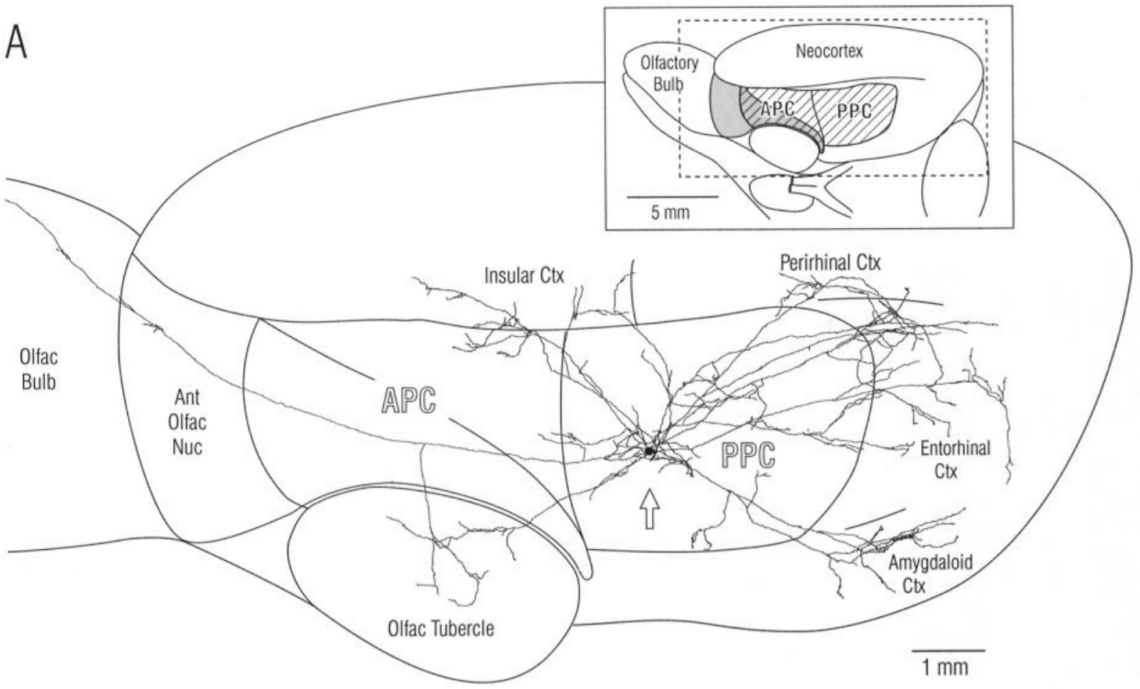

Fig 1.7: Projection Neurons from Piriform Cortex Terminate in Agranular Insular Cortex

Individual piriform neurons were injected with BDA using a sharp electrode and iontophoresis. Reconstruction of the axonal arbor demonstrated projections primarily to other odor cortical areas with the exception of perirhinal/entorhinal cortex and Agranular Insular cortex. (Johnson et al., 2000a)

To test for single cell convergence, we employed a modified conditional rabies viral tracing strategy. First, we infected piriform cortex with AAV carrying the trans-synaptically transported plant lectin WGA fused to a molecule of cre-recombinase (wga-cre) (Fig 1.8A) (Gradinaru et al., 2010; Libbrecht et al., 2017). We simultaneously injected AAV containing a cre-dependent glycoprotein coat and the surface receptor for a modified rabies virus into Agranular Insular cortex, thereby permitting cells which received input from piriform to later be infected with pseudotyped rabies (Fig 1.8B) (Wall et al., 2010; Wickersham et al., 2007). This rabies required the complement of g-protein and thus was only able to retrogradely infect neurons one synapse away (Fig 1.8C). As seen in Fig 1.9, green cells received wga-cre from a distal piriform injection site. Those that were later-co-infected with rabies are yellow while the cells that are only red provide input to yellow cells (Fig 1.9). Although multiple low-probability events are required to co-occur to achieve these results, they demonstrate that individual cells in AIc receive convergent input from piriform and gustatory cortices.

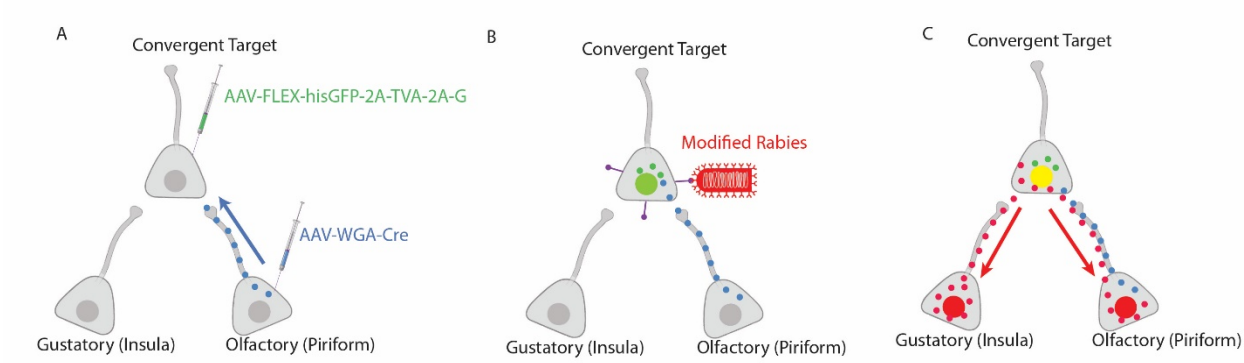

Fig 1.8: Conditional Rabies Tracing Strategy

A. AAV-WGA-cre is injected into piriform cortex and transported (blue dots) anterograde to neurons in AIc. AIc is simultaneously injected with an AAV encoding glycoprotein and the TVA receptor which are only expressed in the presence of cre-recombinase. **B.** Cells in AIc which receive wga-cre from piriform inputs express GFP (green) and the cell surface receptor TVA (purple) which permits infection by modified rabies virus (red). **C.** The rabies virus can infect these starter neurons (now yellow) and because the cell also expresses complementing glycoprotein (green), the virus particles (red) are able to spread retrogradely and infect pre-synaptic neurons (now red).

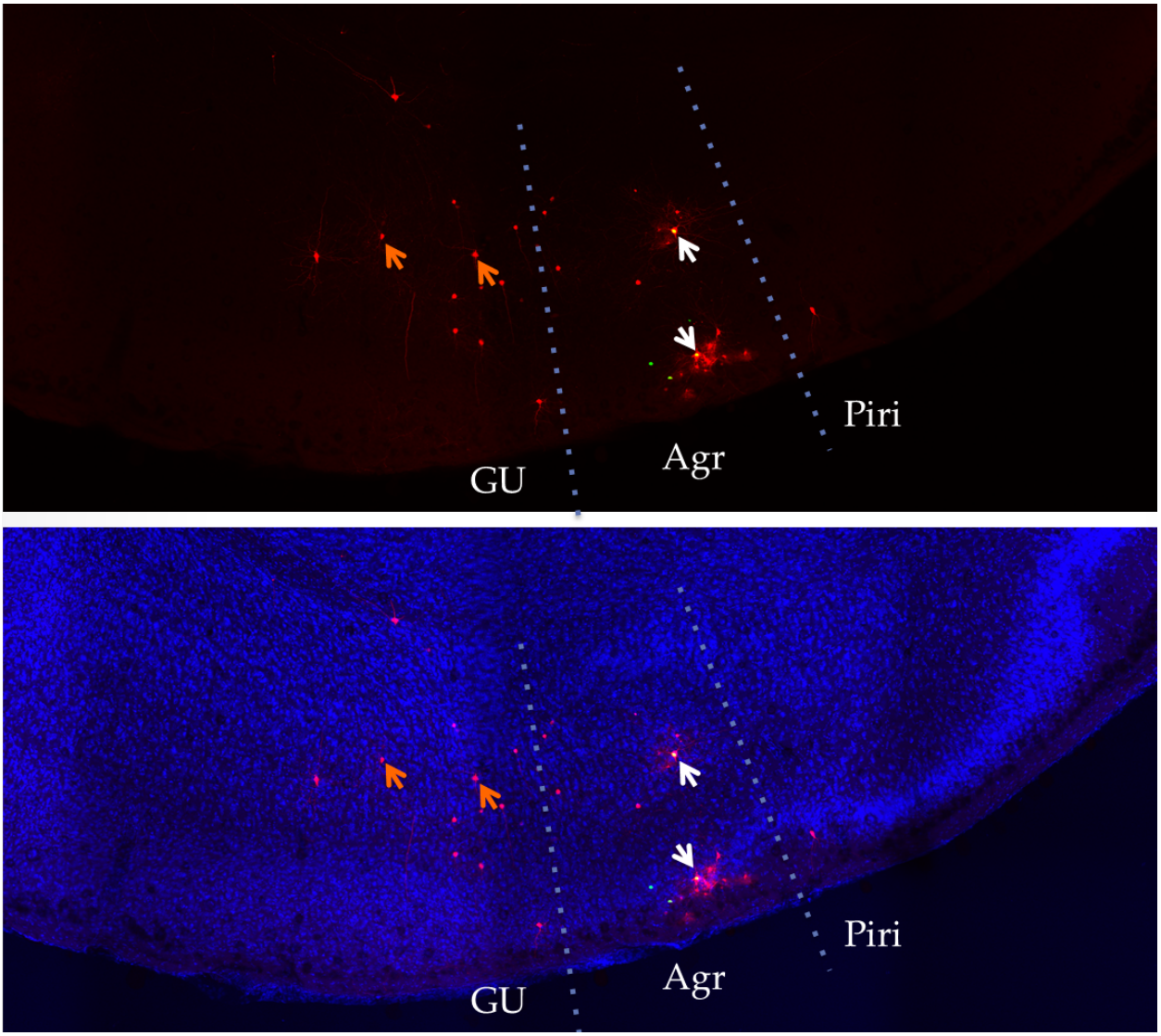

Fig 1.9: Conditional Rabies Tracing Demonstrates Convergent Input from Gustatory and Piriform onto Single Cells in Agranular Cortex

Cells receiving anterograde transported wga-cre are green. Those cells which were then infected with pseudotyped rabies are yellow (white arrows). These seed cells then retrogradely infected subset of their inputs which are only red (e.g. orange arrows). Additional red cells were seen in other slices of Piriform cortex (not shown).

Discussion

From the hand drawn decussation of the optic nerve by Ramón y Cajal to the systematic projection mappings compiled by researchers at the Allen Institute, anatomical characterization of the brain has continued to inform our understanding of its functions (Llinás, 2003; Oh et al., 2014). Building on existing knowledge of gustatory and olfactory sensory systems, we show that agranular insular cortex is the primary site of anatomical taste-odor convergence.

A confluence of inputs emanating from primary sensory areas has been the starting point for exploring multisensory integration in various regions of the brain (Schroeder et al., 2003). Such projections have been observed between primary sensory areas as well as onto liminal regions between sensory areas (Ghazanfar and Schroeder, 2006; Wallace et al., 2004). Similar interrogation of gustatory and olfactory anatomical convergence has been limited by the techniques available. Early studies using WGA-HRP generally localized the site of convergence to insular cortex (Shipley and Geinisman, 1984) while subsequent studies have traced these distinct pathways to AIc (Johnson et al., 2000b; Shi and Cassell, 1998b). This coarse grain anatomical evidence has even been used to argue for AIc as the site of taste-odor integration (Sewards and Sewards, 2001).

We found that piriform and gustatory cortex have convergent synaptic input onto individual cells. The anatomical convergence of odor and taste inputs in the AIc could be seen as the probabilistic result of dense local projections, or as a specific target with a unique functional role in integration. In our experiments, the distances between piriform inputs (injected with wga-cre) and the convergent cell targets were greater than 1mm, a distance at which the probability of connectivity is low (Ercsey-Ravasz et al., 2013; Perin et al., 2011). This long-range cortico-

cortical connectivity matches the arborization seen in reconstructions of piriform cell morphology (Johnson et al., 2000b).

It should be noted that while our modified rabies strategy identifies single cell targets of convergent input with fine resolution, it suffers from inefficiency at multiple stages. An alternative approach to synaptic convergence was also considered (Hooks et al., 2015; Yizhar et al., 2011). In these experiments, one could express a blue light activated opsin in piriform cortex and a red light activated opsin in gustatory cortex. Whole cell patch clamp recordings in AIc could then be combined with artificial activation of odor and taste inputs to survey the probability of connectivity. Future work could use this strategy to more thoroughly quantify the probability of convergence which we show here.

Experimental Procedures

Animals

Experiments were carried out using 8 - 12-week-old C57BL/6J mice; all animal care was in accordance with institutional guidelines. Prior to injection mice were anaesthetized with ketamine and xylazine (at a ratio of 100 / 10 mg per kg). Mice were placed on a custom-built stereotaxic frame and core-body temperature of anesthetized animals was maintained at 37 ˚C using a feedback-controlled heating pad.

Viral Tracing

Viral constructs were loaded a pulled glass capillary needle and injected unilaterally. For basic projection tracing, 80nL of 1:1 AAV2/1 CAG-FLEX-tdTom + AAV2/9 CMV-Cre into anterior insular cortex (+1.1 AP, 3.7 ML, 2.2 Z) or AAV9.eGFP.WPRE.bGH into posterior piriform cortex (-0.7 AP, 3.8 AP, 4.5 Z). Animals were perfused for tissue processing ~3 weeks after the AAV injection.

For rabies based tracing, animals were simultaneously injected with ~50nL of AAV-Cre-GFP into posterior piriform cortex and ~50nL of AAV-FLEX-hisGFP-2A-TVA-2A-G into anterior insular cortex. The mice were allowed to recover and after 6 weeks (to permit trans-synaptic transfer of wga and subsequent expression of surface receptor TVA), a second injection following the same protocol was made into approximately the same anterior insular cortex location where ~100nL of EnvA-SADΔG-mCherry was injected. The animals were perfused for tissue processing 10 days after the rabies injection.

Chapter 2

Calcium Imaging of Odor-Taste Mixtures in Agranular Insular Cortex

Introduction

Our current understanding of chemosensory representations in cortical brain areas has been advanced by the use of calcium imaging to characterize the response properties of large populations of cells with single cell resolution. These experiments have demonstrated that the spatial organization of activity corresponds to proposed functions of these systems. Specifically, the olfactory cortex serves as a labile associative region with no innate meaning, but with the ability to pair odor with outcome through plasticity (Choi et al., 2011; Gore et al., 2015). Correspondingly, responses to various odors are distributed throughout piriform cortex with substantial overlap (individual cells have responses to multiple odors). In contrast, taste cortex appears to be hardwired with an anterior-posterior axis of valence (it is unclear whether this axis is continuous or discontinuous) such that anterior regions specifically respond to sweet and posterior regions respond to bitter(Chen et al., 2011). These imaging studies referred to the rhinal vein as roughly demarcating the border between primary taste and olfactory cortices and thus providing a visual target for recording in Agranular cortex.

Despite a broad interest in odor-taste integration, there is little evidence for a functional site of integration. The most established research come from single cell recordings in primates demonstrating cells in orbitofrontal cortex (OFC) that respond to both odors and tastes, but it is known that AIc projects to OFC and thus integration could be happening earlier (Rolls and Baylis, 1994). More recent studies in rodents have used separate presentations of odor and taste in insular and piriform cortices, finding populations of cells that respond to both odor and taste

(Maier et al., 2012; Samuelsen and Fontanini, 2017). In all these studies, the cells which respond to odor and taste appear to be broadly tuned to various stimuli from each modality. Moreover, none of these studies look at simultaneous presentation of odor and taste to distinguish the compound stimulus response from the component stimuli. Here, we present the results of recordings from close to 10,000 cells sampled from dozens of animals. These experiments demonstrate that agranular insular cortex has responses to odor taste combinations which are distinct from the component stimuli and which are altered by experience.

Experimental Setup

Using mice with constitutively expressed Ca^{2+} indicator (see methods), anaesthetized animals were double-tracheotomized and head fixed before creating a cranial window around the intersection of the MCA and rhinal vein. This region lies in the center of a previously identified taste region while being closer to piriform cortex. Mice were then tested with a panel of odor(s), taste(s), or a combination of odor/taste (summary of individual responders in Fig 2.16).

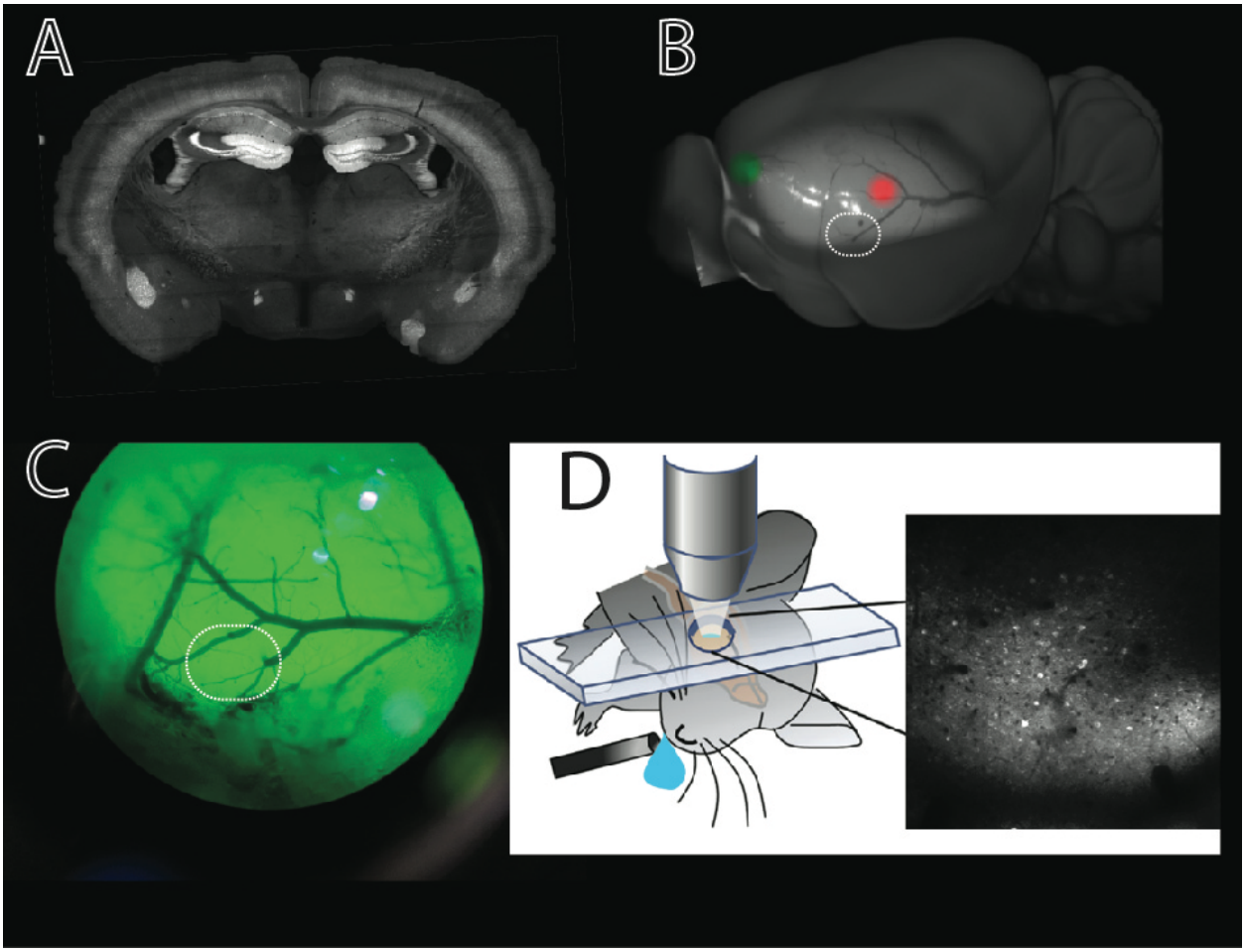

Fig 2.1: Calcium Imaging in Agranular Cortex

A. Coronal slice from a transgenic mouse expressing Gcamp6s under the control of the Thy-1 promoter have expression in a random set of excitatory neurons. **B and C.** Vasculature can be used to approximate the location of AIc. Generally, regions surrounding the intersection of the lower branch of the rhinal vein (running horizontally in B and C, and the MCA (running nearly vertical) were targeted for recording. **D.** Anaesthetized and double-tracheotomized mice had a cranial window exposed and were placed under a 2-photon microscope while tastants were delivered to the mouth and/or odorants were delivered retronasally.

Results

The first question we wanted to answer was: how are tastes represented in AIc? While 2-photon imaging in granular cortex demonstrated spatial segregation in a gustotopic map, the initial tracing from granular cortex suggested that a given taste region projects diffusely throughout AIc. Are taste responsive neurons selective for one taste or broadly tuned?

Taste responsive neurons were distributed in a salt and pepper fashion with a given field containing both sweet and bitter responsive cells (Fig 2.2A) though few cells responded to both bitter and sweet (Fig 2.2B, example traces in Fig 2.3 B, C). This separation of taste responders was seen across animals (Fig 2.2B, Fig 2.3A). Taste responses were reliable across multiple trials spanning several hours of imaging (Fig 2.3 C, Fig 2.17).

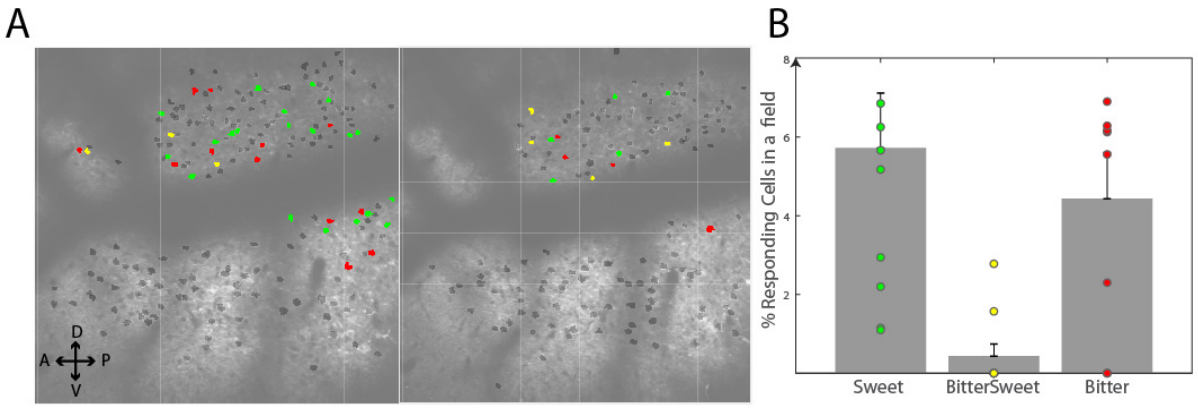

Fig 2.2: Taste Responsive Cells Are Intermingled but Segregated

A) Two planes from a single animal show no obvious spatial organization of sweet (green), bitter (red) or bitter/sweet (yellow) responders. **B.** This intermingled segregation was seen across all animals in which bitter and sweet were tested (n=10 planes from 5 animals).

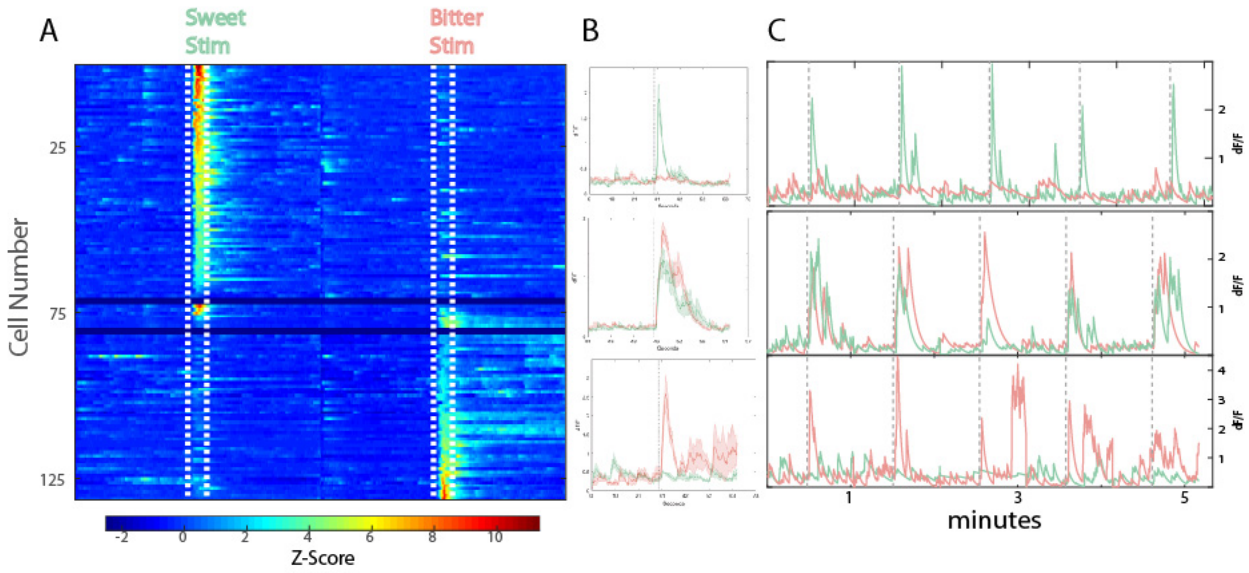

Fig 2.3: Taste Responses Are Reliable Across Trials

A. Heatmap of all bitter and/or sweet cells. Mean responses were z-scored across all stimulus conditions; dotted white lines show 5s stimulus window. **B.** Examples of sweet-only (top), bitter-sweet (center), and bitter only (bottom) responders (bitter=red, sweet=green, mean +/- s.e.m.). **C.** First five trials for bitter and sweet of cells shown in B; dotted lines show stimulus onset.

We next asked whether odor responsive cells are intermixed with taste cells, as tracing would suggest. Indeed, while there was a bias towards taste representations in dorsal regions and odor representations in ventral regions, these populations are intermixed within AIc (Fig 2.4 A). We also found mixture responsive cells when taste and odor are simultaneously delivered to the animal (Fig 2.4 B, C). This population includes cells that respond to individual components as well as cells that selectively respond to the mixture (Fig 2.4 D). These mixture only responders span the dorsal-ventral axis without any apparent spatial organization (2.4 B, un-circled dark cells).

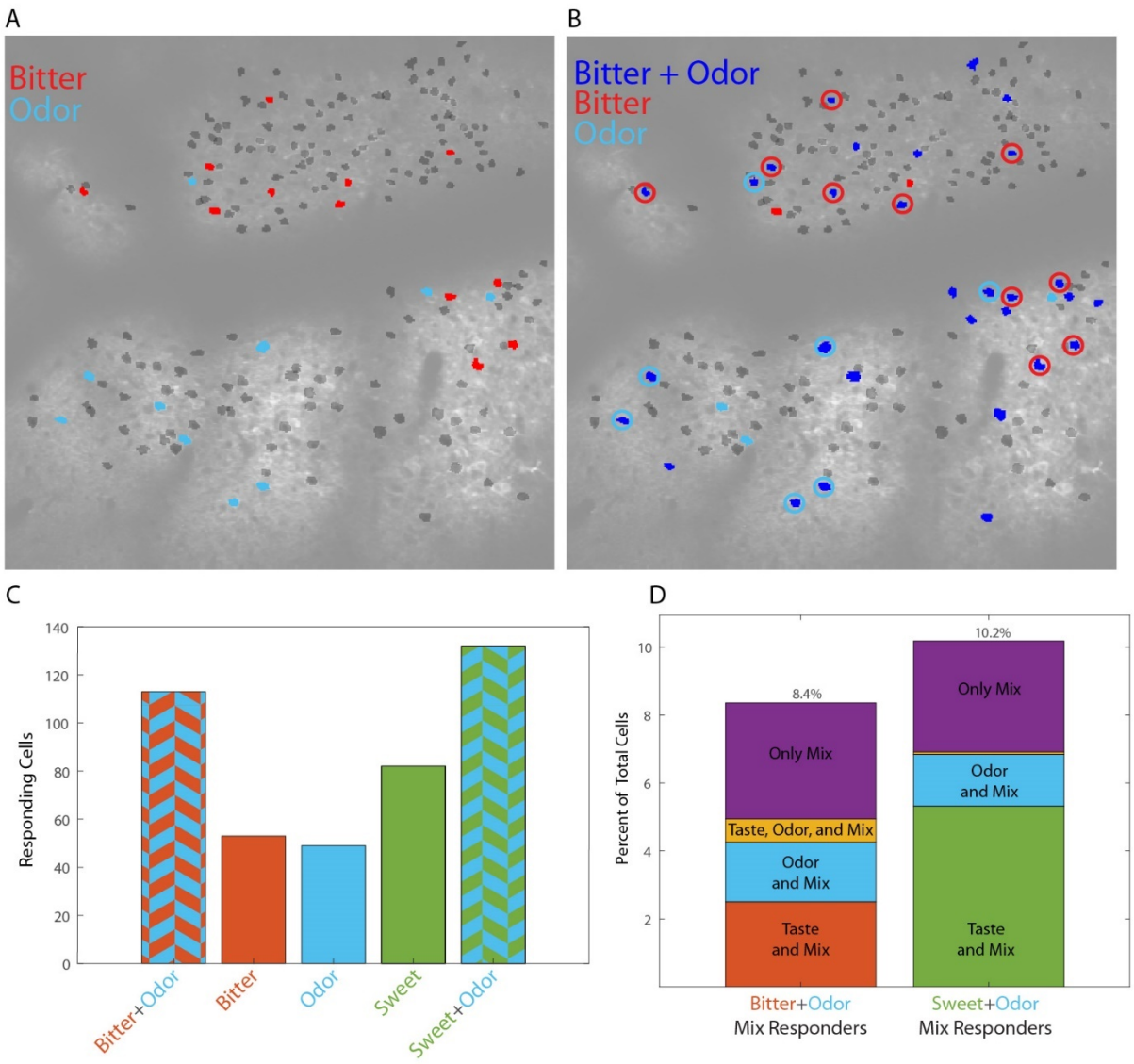

Fig 2.4: Taste, Odor, and Mixture Responders

A. Imaging field showing Bitter (red) and Odor (light blue) responding cells. **B.** The same field now with Bitter+Odor (dark blue) responding cells superimposed. Circled mix responders also respond to the component matching the circle color while dark blue cells with no circle only respond to the mixture. **C.** Number of cells responding to different stimuli (n=5 animals, 10 planes). **C.** Breakdown of mix responding cells by their response to component stimuli.

To elucidate the differences between population responses to different stimuli, we created a pseudo-population of trial-by-trial responses by combining data from responding cells from a cohort of animals tested with bitter, sweet, odor, bitter+odor, and sweet+odor (odor = n-amyl acetate)(Fig 2.5A). These high-dimensional responses were then projected onto their first three principal components (Fig 2.5B). As expected, bitter and sweet are segregated both from each other and from odor responses. Intuitively one might expect that the mixture would lie in a space between the component stimuli but in fact the mixture trials are further from all other stimuli (Fig 2.5A, B). This suggests that pairing tastes with odors could increase discriminability.

We next wanted to ask how odor is represented in AIc. Previous work has demonstrated spatially distributed and overlapping ensembles of piriform cortex neurons that respond to odor. These experiments have all used orthonasal presentation of odor, in line with sniffing behaviors. Since we are interested in odor as it relates to the creation of flavor, we delivered odors retronasally. In contrast to the distinct segregation seen in bitter and sweet responses (Fig 2.2 A,B), multiple odors broadly overlapped (2.6 A,B,C) as seen in the heatmap of responses to amyl acetate (odor1) and ethyl butyrate (odor2), two esters which are neutral to naive animals (Root et al., 2014). Projecting these responses onto PCA space, we see that overlapping odor trials increase their distance when paired with taste (Fig 2.6 D, E).

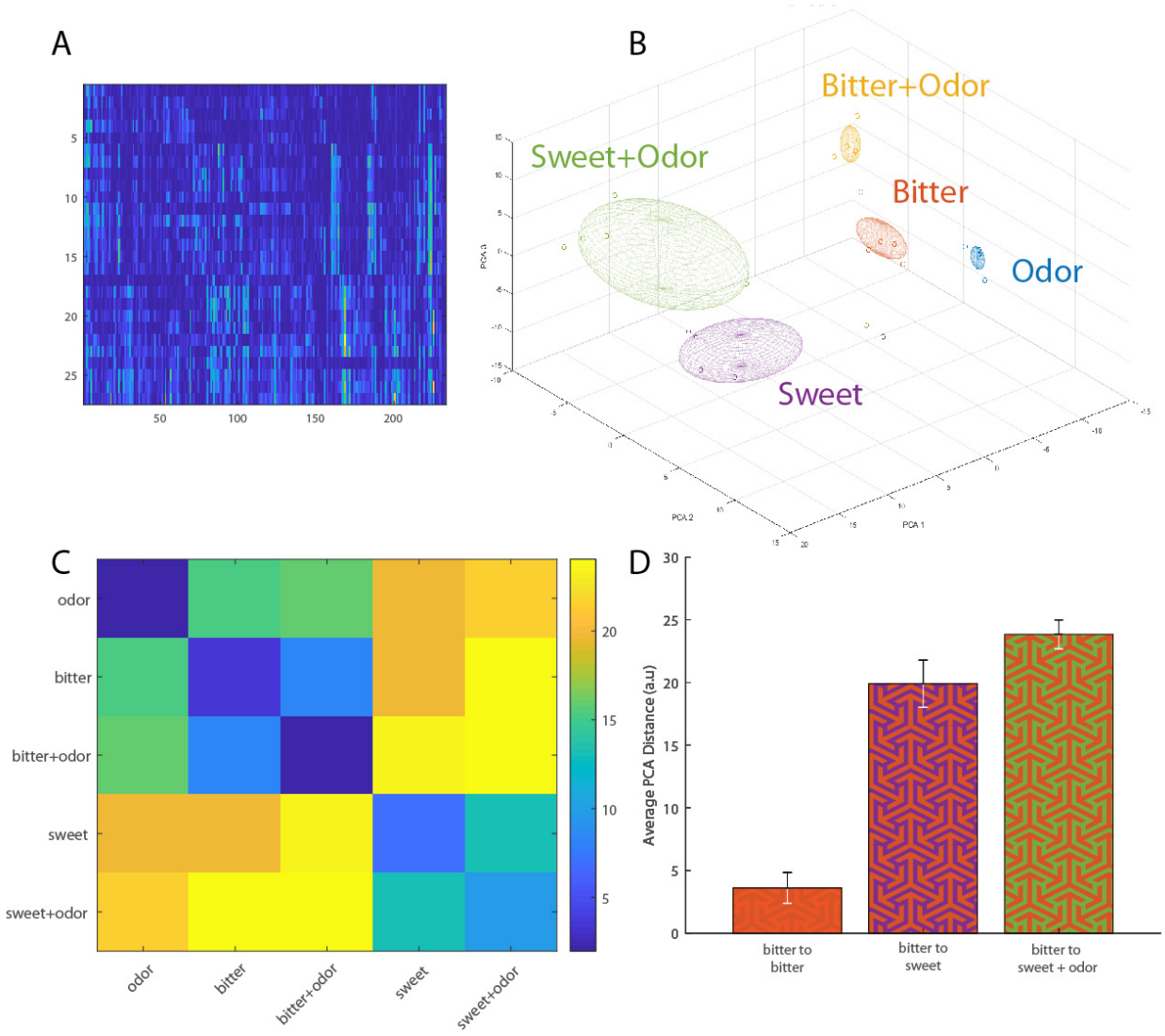

Fig 2.5: Separation of Population Responses in PCA space

A) Responses for all trials (z-scored across trials) from cells that responded to any of the stimuli. **B)** Individual trials (small filled circles) projected onto the first 3 PCA axes. Ellipsoids show mean +/- 1 s.d. **C)** Matrix of average distance of trial points within (along diagonal) and between stimuli. **D)** Bar plot showing average distances for three of the comparisons from C.

.

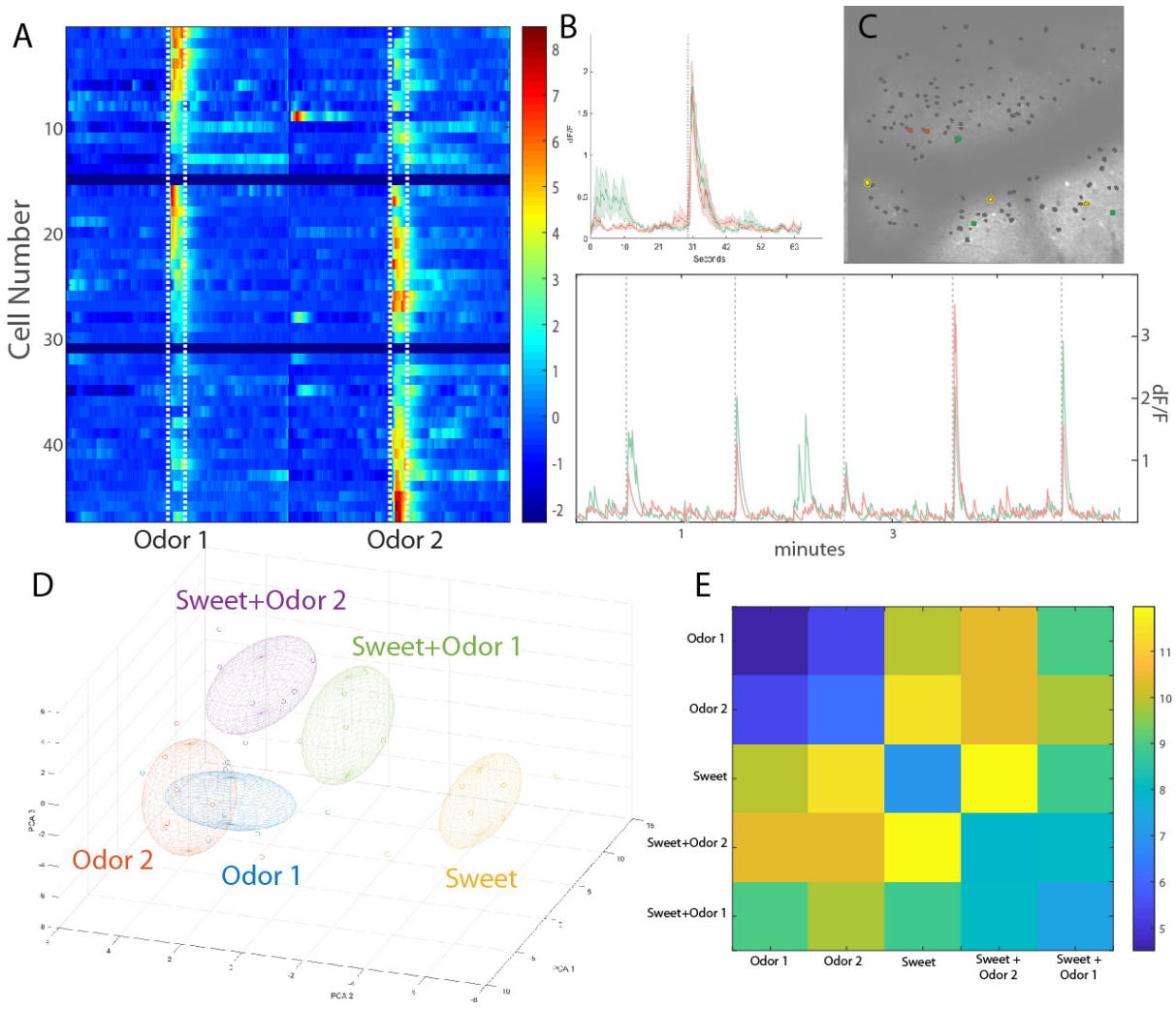

Fig 2.6: Odor Responsive Cells Overlap

A. Heatmap of all ethyl-butyrate or amyl-acetate responding cells (combined from 8 trials, 4 animals). As before, mean responses were z-scored across all stimulus conditions; dotted white lines show 5s stimulus window. **B.** Example response from "dual" responder showing mean +/- s.e.m traces for isoamyl (green) and ethyl-butyrate (red) (top) and single trial traces (bottom); dotted lines show stimulus onset. **C.** Overlap of odor responsive cells in an example plane. **D, E.** Individual trials projected into PCA space and calculated distances as in 2.5 C, D.

While reducing the dimensionality of the datasets can provide insight into how population activity is shifting between stimulus conditions, it leaves open the question of how individual cells' activity is changed by multisensory stimuli. We know that the number of cells responding to *both* odor and taste, according to the classification criteria used, is a relatively small portion of the population. However, multisensory cells which appear tuned to an individual modality could be modulated by a compound stimulus.

Previous work on multisensory integration has focused on the response to mixtures relative to the responses to component stimuli. An "additivity index" is formulated as:

$$Rm/(Rc1 + Rc2)$$

where *Rm* is the response to mixture, and *Rc1* and *Rc2* are responses to component stimuli. This treats linear summation as a default, giving an index of 1. Examples of super-additive (index>1), additive (index ~1) and sub-additive (index<1) responses can be seen in Figure 2.7. By calculating the range of indices for the same dataset presented in Figure 2.5, we can see that the median index is slightly suppressive while there is a long tail of superaddtive cells (Fig 2.8). Notably, most cells do not have an index of 1, demonstrating that there is multisensory modulation of responses in AIc. Similar distributions can be seen in animals probed with sweet combined with two neutral odors (Fig. 2.10). We next looked at additivity index for different groups of mixture responsive cells, separating them by their responses to components. We found that cells responding only to the mixture comprise the long tail of additivity, demonstrating that this population is distinct from unisensory responders (Fig. 2.9).

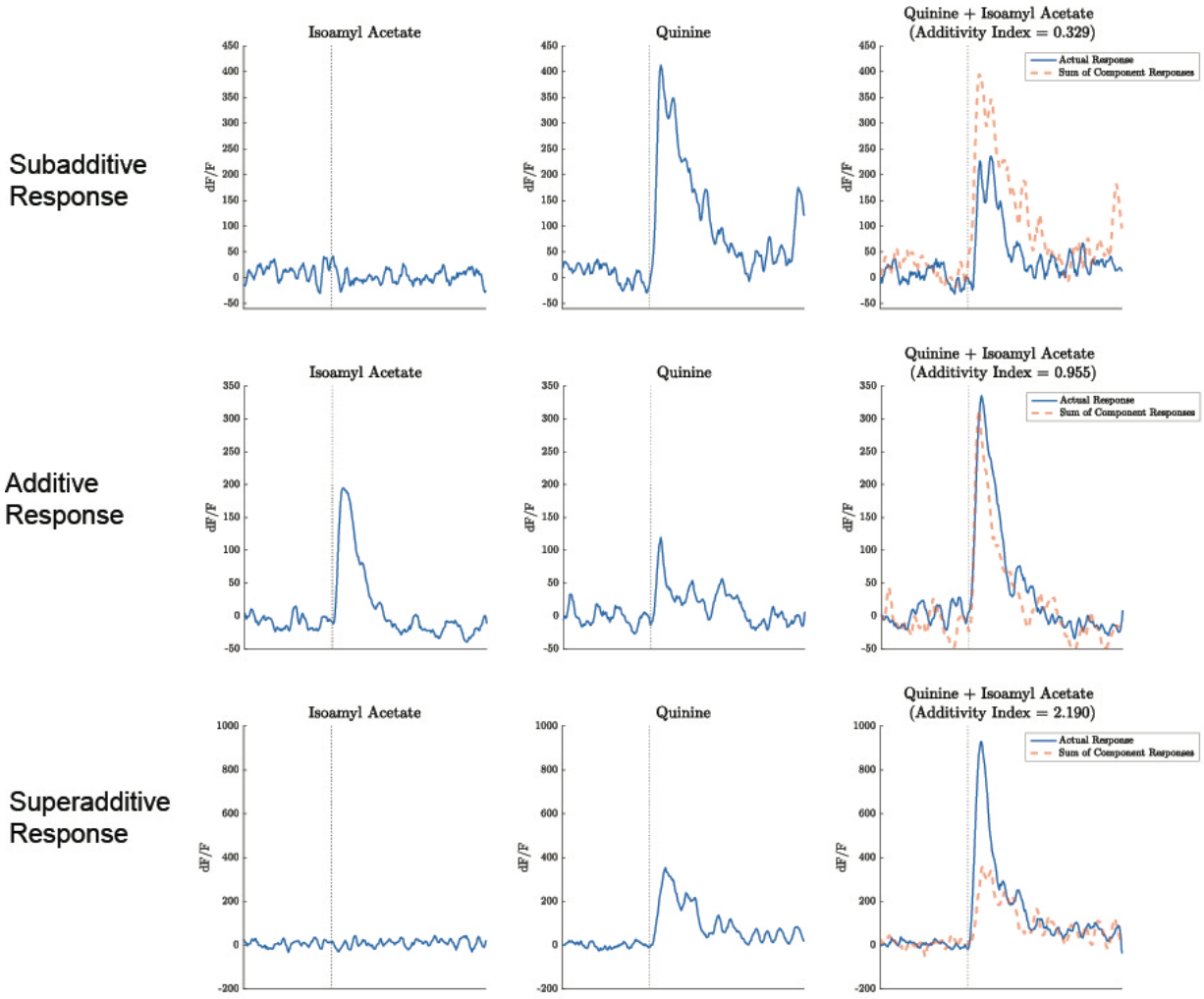

Fig 2.7 Single Cell Integration Index Calculations

Shown are hypothetical sums of component stimuli responses with the actual mixture response. Additive responses reflect a response to the mixture which approximates a linear summation of responses to the component stimuli while subadditive and superadditive responses reflect non-linear suppression or enhancement respectively.

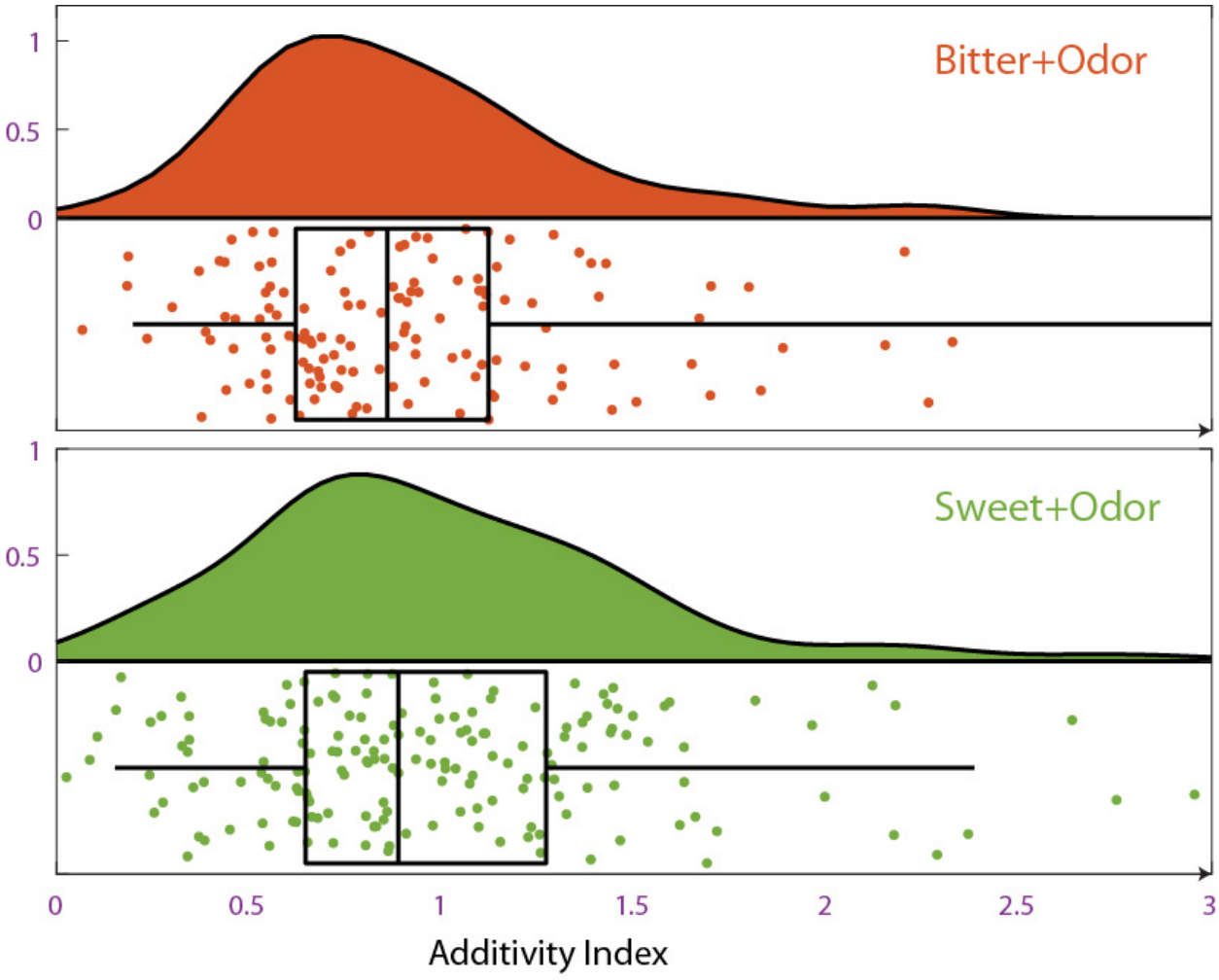

Fig 2.8: Distribution of Additivity Indices of Bitter+Odor and Sweet+Odor Cells

Individual points are single cell additivity indices. Region above abscissa contains probability density.

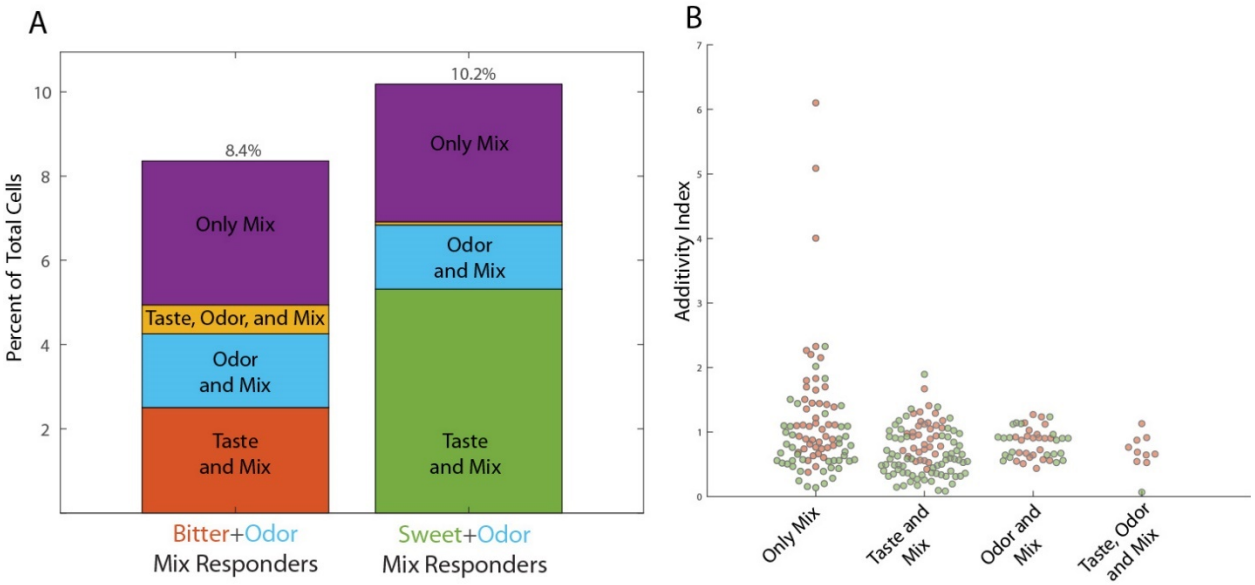

Fig 2.9: Additivity Indices for Mixture Responsive Subcategories

A. Breakdown of mixture responsive cells into subcategories (as shown in 2.4D). **B.** Additivity indices for different subcategories of mix responsive cells. Red circles are indices of Bitter+Odor responsive cells while green circles are Sweet+Odor responsive cells.

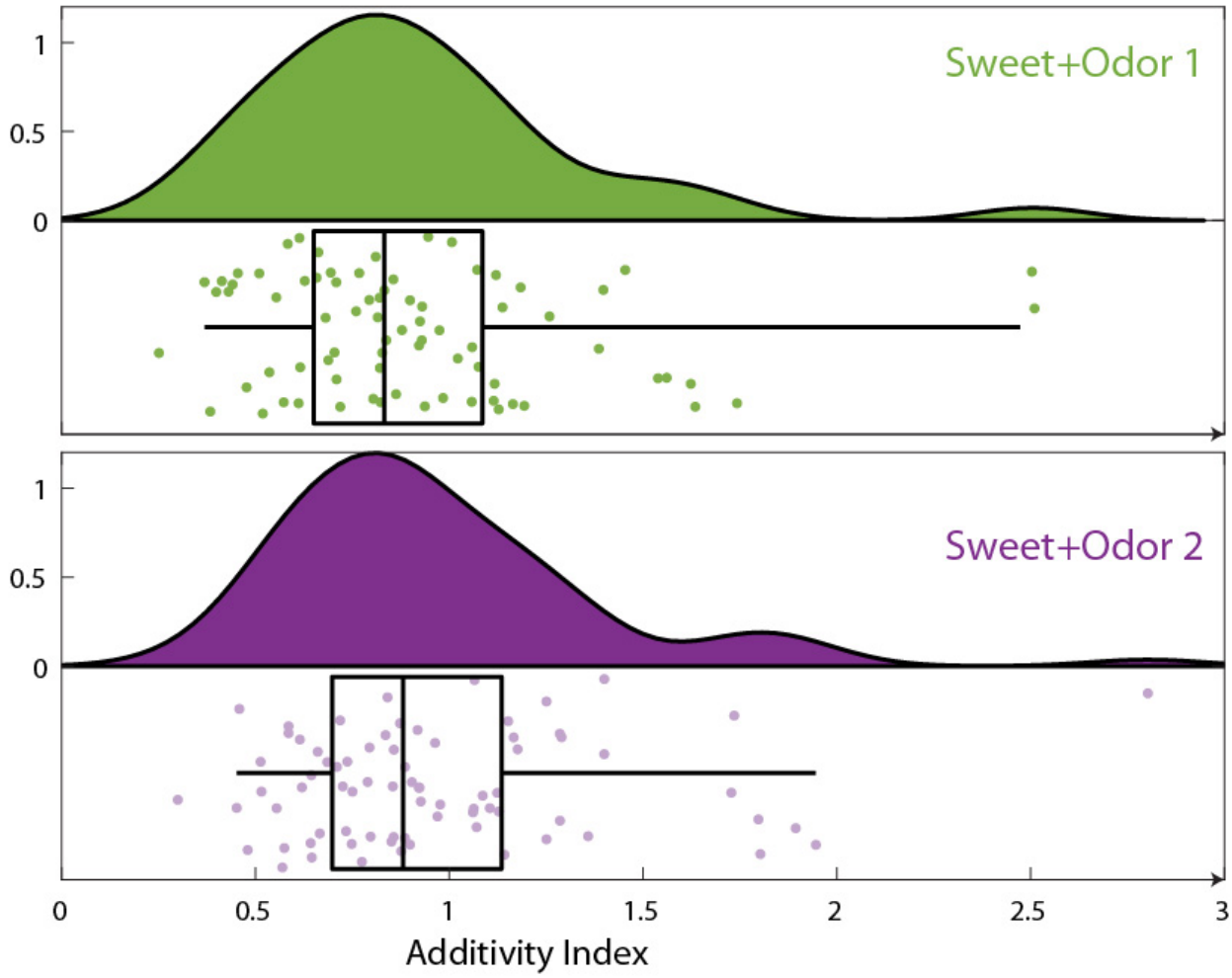

Fig 2.10: Distribution of Additivity Indices for Sweet Mixtures with Two Different Odors. Individual points are single cell additivity indices. Region above abscissa contains probability density.

Experience Modulation of Odor-Taste Integration

One interpretation of the similarly distributed additivity indices is that the innate connectivity in AIc is random and thus gives rise to a spectrum of responses which can then be shaped by experience. In the superior colliculus, cells responding to audio and visual input demonstrate a shift in their additivity index following repeated presentations of paired stimuli (Stein et al., 2014). In human experiments, the reported intensity of a novel taste-odor pairing increased after repeated exposure (Fig 2.11) (Prescott, 2012). To test whether experience would alter integration in AIc, we turned to a flavor conditioning task in which the animals develop a preference for caloric flavors over non-caloric but equally sweet flavors (Sclafani et al., 2010).

Naive mice were first presented with two bottles, containing either grape or cherry flavored water (Fig 2.12 A). The less preferred odor was then paired with the caloric sweetener sucrose while the initially preferred odor was paired with the artificial sweetener sucralose. The sweetener concentrations were matched to initially be equally attractive (Fig 2.12 B). Following repeated exposures to one mixture at a time, mice develop a strong preference for the caloric mixture (Fig 2.12 C) ($n=3$, $p = 0.04$, two-sample t-test). This preference extended to flavored water (Fig 2.12 D) ($n=3$, $p<0.001$, two-sampled t-test). We then asked whether a divergence in flavor responses between the preferred and non-preferred mixtures could be seen using calcium imaging.

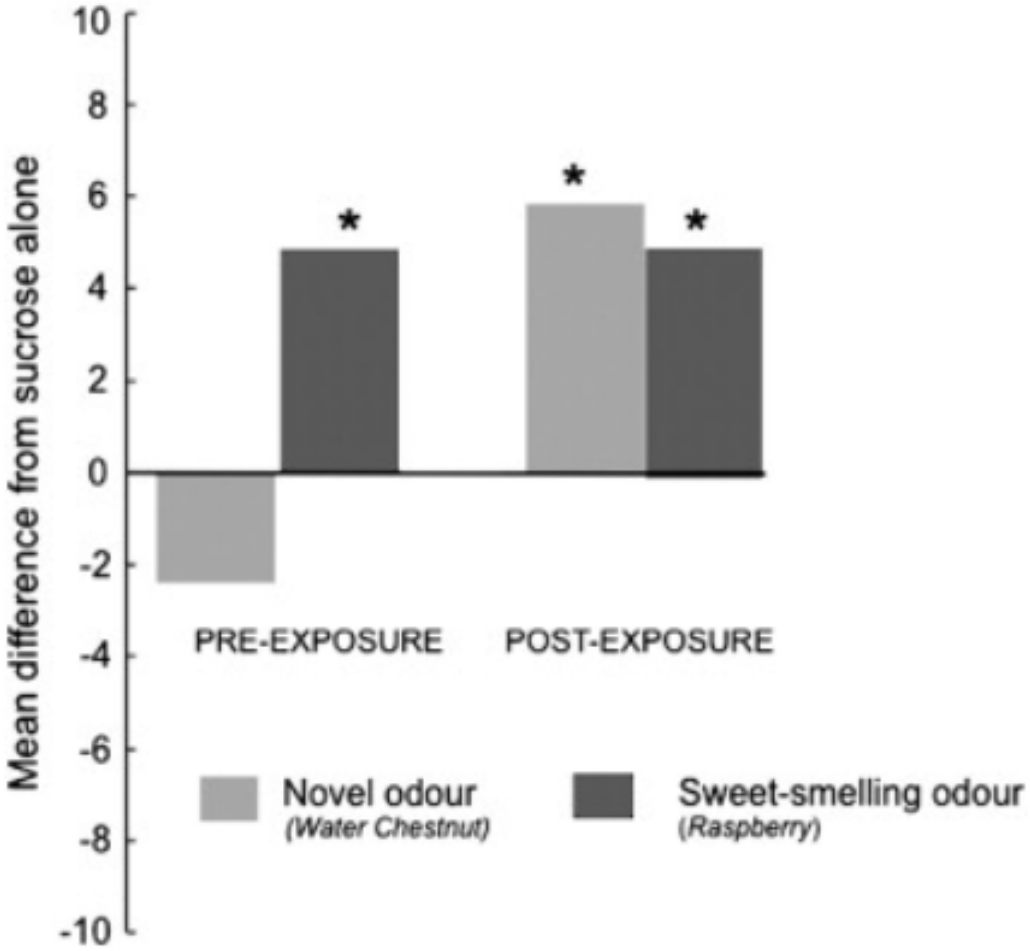

Fig 2.11: Experience Enhances Perceived Intensity of a Flavor in Humans

A novel taste-odor mixture (sucrose + water chestnut) was initially perceived as no different from the taste alone. Following repeated pairing of the taste and odor, subjects reported the mixture to be significantly sweeter than the taste alone (Prescott, 2012).

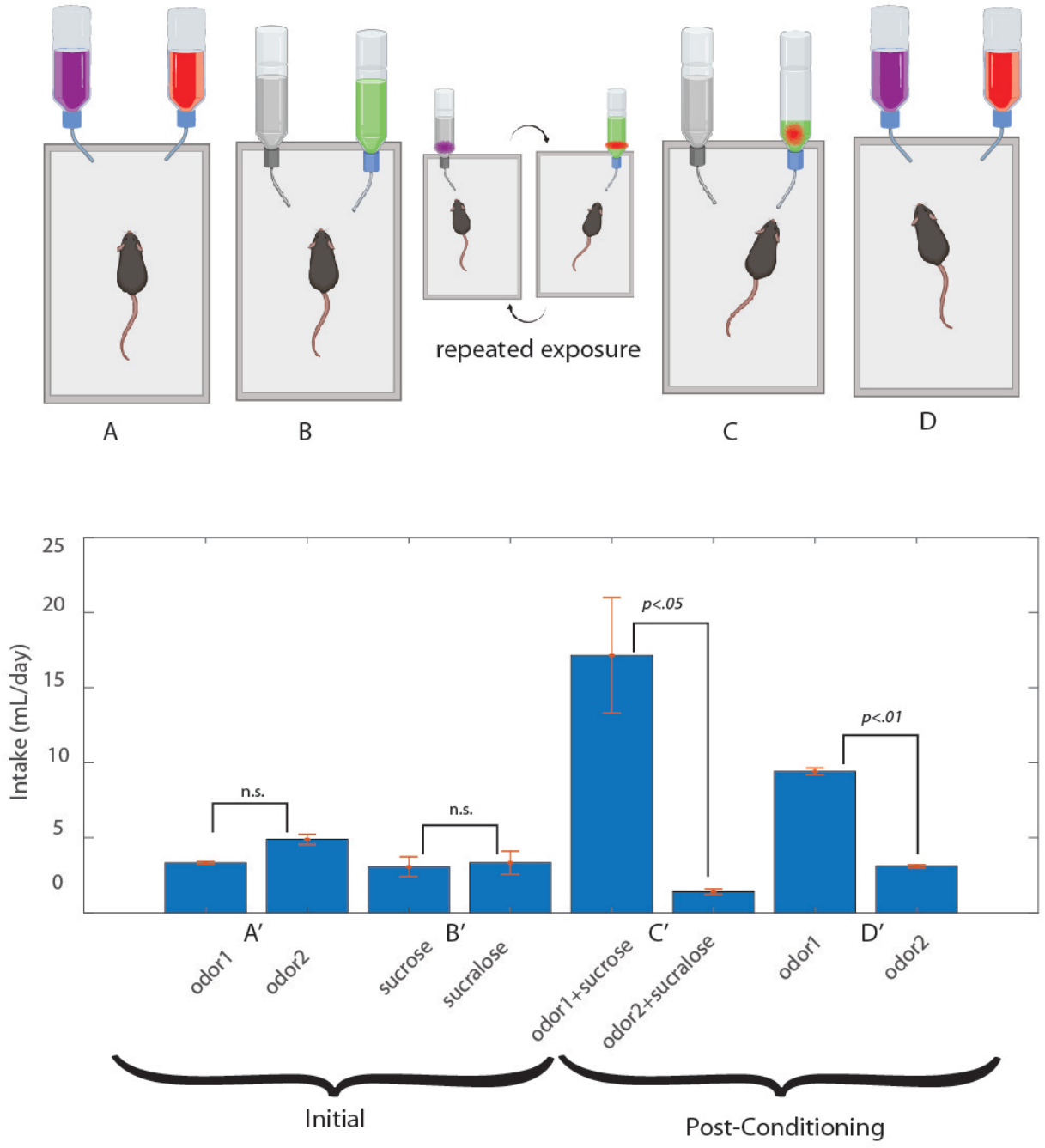

Fig 2.12: Flavor Conditioning Paradigm and Resulting Preference

Upper cartoon shows presentations corresponding to volumes consumed in lower bar chart. **A.** Two odors in water. **B.** Non-Caloric (grey) vs. Caloric (green) sweetener. Center cartoon shows repeated presentations of caloric and non-caloric odor-sweet pairings. **C.** Post-Conditioning

consumption of caloric and non-caloric mixtures. **D.** Testing of odors in water after conditioning.

As seen in Figure 2.13, there are no differences between the caloric flavor and non-caloric flavor. This is consistent with the idea that the odor itself serves as a conditioned stimulus while the nutritive content (not the sweetness) of the solution acts as an unconditioned stimulus (Touzani and Sclafani, 2007). The sweet region of gustatory cortex responds similarly to both caloric and non-caloric sweeteners, so it is unlikely that this association is occurring in AIc (Chen et al., 2011).

We next asked whether the repeated pairing of sweeteners with odors affected neural responses by comparing them to naive animals. Here, we analyzed the data across naive and conditioned animals, looking at responses to sweet and odor pairings. As seen in other multimodal regions, there is a shift in the distribution of indices with experienced animals' integration indices being closer to additive (Fig 2.14) ($p<0.001$, Wilcoxon rank sum test). In naïve animals, most super-additive cells responded only to the mix (Fig 2.9B). Since the distribution of additivity indices was shifted to the right in experienced animals, we asked whether there was an increase in the population which responds only to the taste-odor mix compared to naïve animals. Indeed, we found a significant increase in the population which responded only to the taste-odor mixture (Fig 2.15) (both flavors experienced vs. naïve $p=.002$, Wilcoxon rank sum test). This change was not seen in mixture responders that also responded to sweet alone.

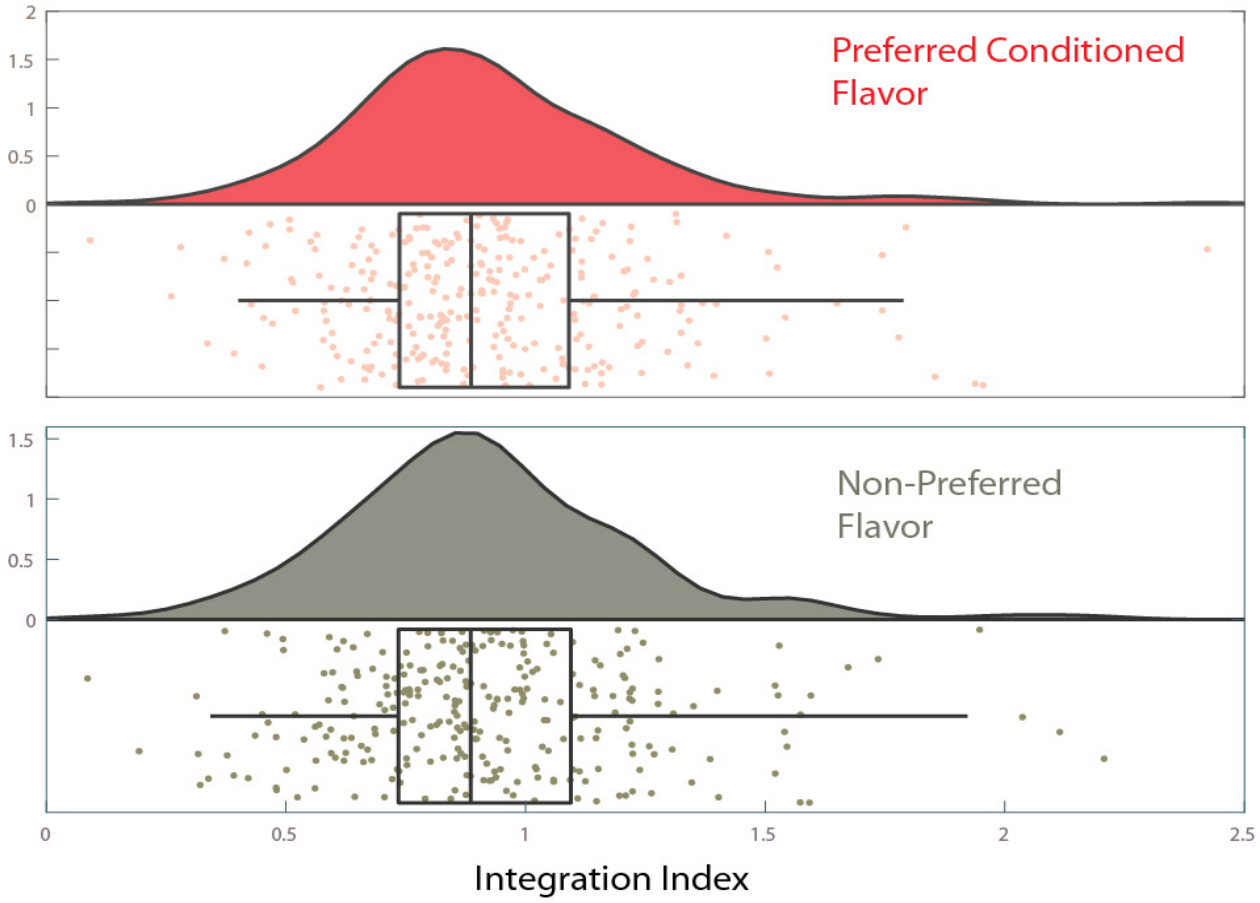

Fig 2.13 Distribution of Additivity Indices for Flavors after Sucrose Conditioning

Individual points are single cell additivity indices. Region above abscissa contains probability density. Following repeated exposures, animals developed a preference for a flavor containing sucrose over a flavor sweetened with the non-caloric sweetener sucralose.

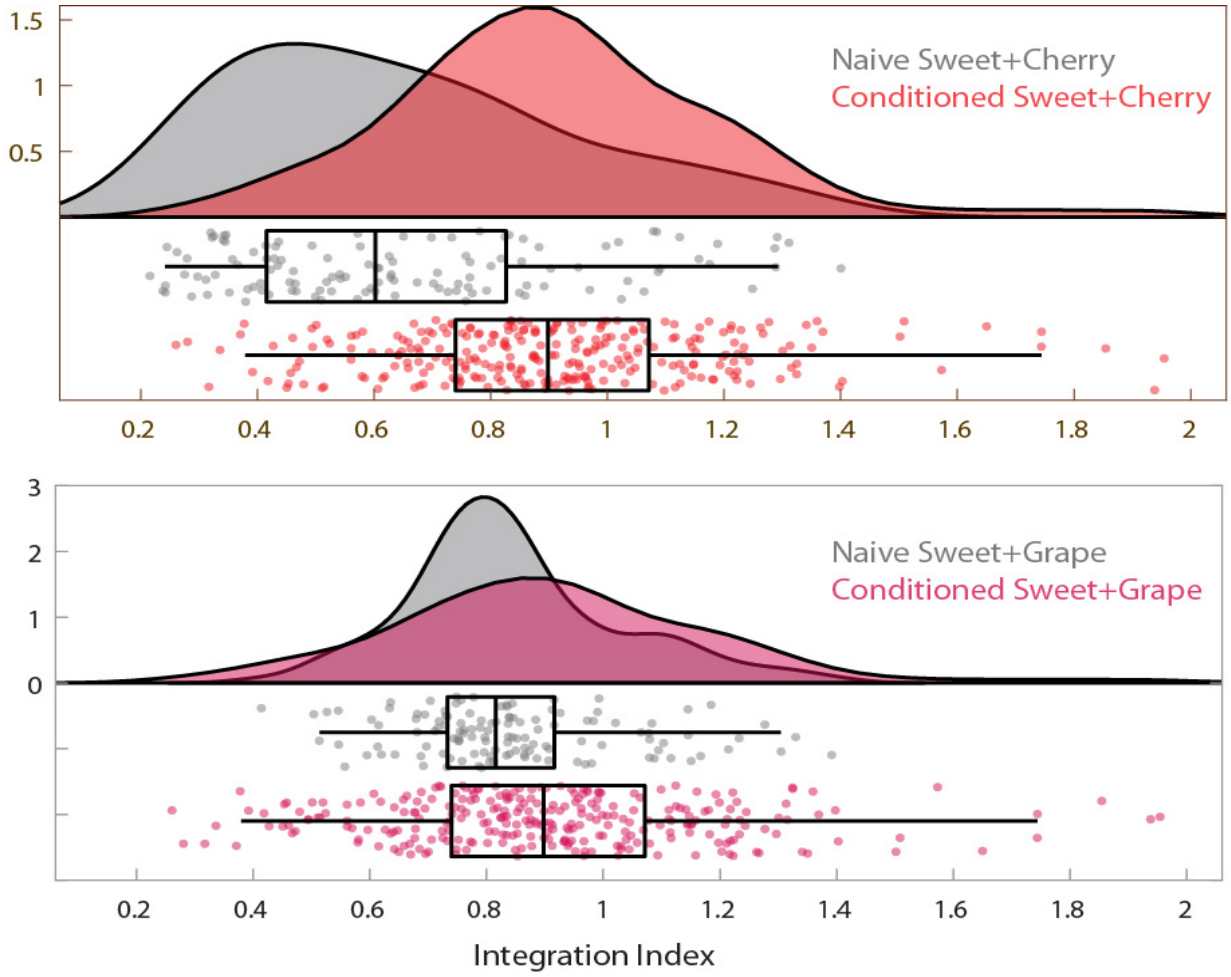

Fig 2.14 Distribution of Additivity Indices of Two Flavors in Naïve and Conditioned animals.

Individual points are single cell additivity indices. Region above abscissa contains probability density. In both plots the colored dataset comes from animals that had repeated exposure to the taste-odor mixture.

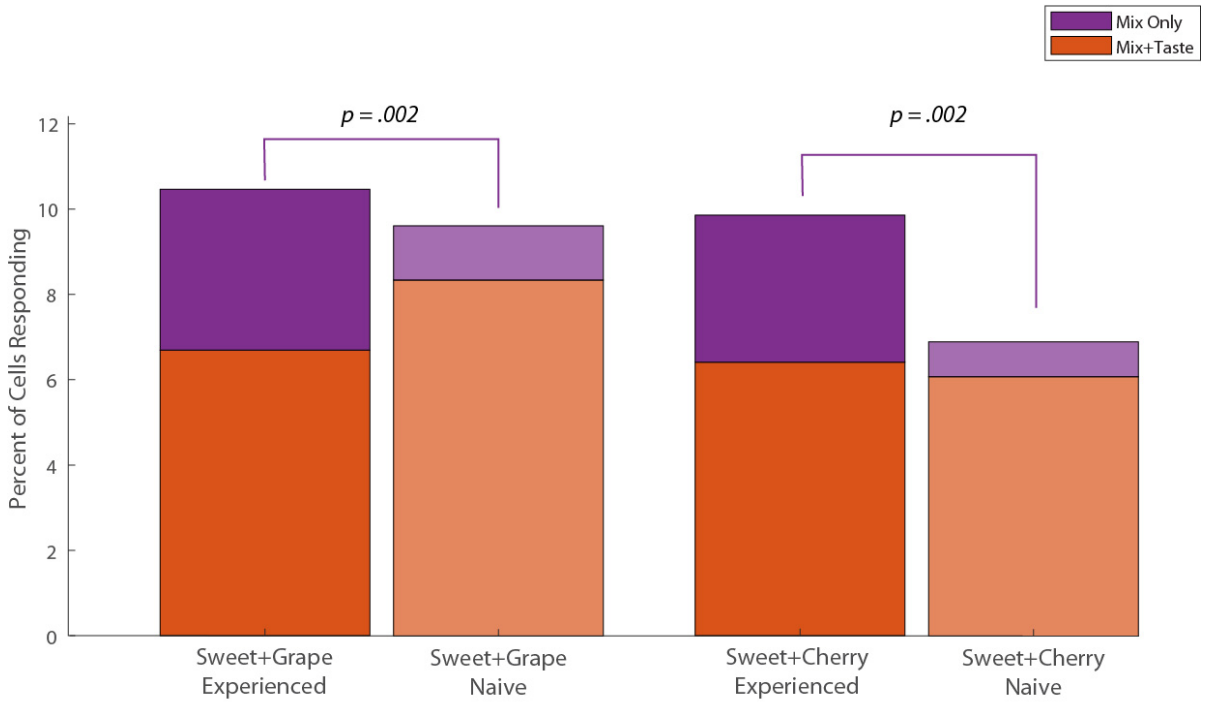

Fig 2.15 Experienced Animals Have an Increase in Mix Only Responding Cells

Mixture responding cells broken down by their responses to component stimuli for two flavor pairings in experienced and naïve animals. For both flavors, the percent of cells responding to only the mix and not the components (purple) is larger in experienced animals (n = 12 fields experienced, n = 6 fields naïve, Wilcoxon rank sum test).

Discussion

Building from the anatomical evidence of integration in AIc, we sought to characterize taste-odor integration with single-cell resolution. We found that taste and odor are represented in the AIc and that flavor mixtures alter populations both by modulating the responses of odor and taste responsive cells while also recruiting neurons that do not respond to either of the component stimuli but do respond to the mixture. This integration of taste and odor is altered by experience, which increases the population of cells that only respond to the mixture.

Previous studies of flavor have sought evidence of taste-odor integration by looking for cells that respond to taste and odor presented separately (Desgranges et al., 2010; Maier et al., 2012), but our results suggest that this approach cannot understand the fundamental transformation that occurs when these stimuli are presented together. We found a relatively small number of cells that responded to both taste and odor alone and note that there are several possible reasons for this. The first is that the olfactory chemical space is vast, estimated at 400,000 different detectable molecules (Mori and Yoshihara, 1995), while the activation of piriform cells by any one odorant is sparse (Roland et al., 2017; Stettler and Axel, 2009). The nature of our experiments constrained the number of odors we could test in any one animal (at most 3 were used), thus limiting the perceptual space that we could sample. The second consideration is our mode of delivery. We delivered odorants retronasally, in following with the processes that create flavor and the evidence from Human studies showing that the unified perception of a flavor is specific to retronasal olfaction (Small, 2012). However, in rodents, retronasal olfaction evokes weaker responses in the olfactory bulb compared to orthonasal

delivery of odorants (Furudono et al., 2013). Future work could more thoroughly evaluate AIc odor responses by testing a broader array of odors and concentrations.

We used an additivity index to characterize how mixture responses differed from responses to component stimuli. This interpretation of single neuron responses originated in superior colliculus where super-additive responses are often seen and thus superadditivity has become a qualifying property of multisensory integration (Stein and Stanford, 2008). However, subadditive integration in visual-vestibular multisensory neurons is associated with near-optimal behavioral performance and a reframing of integration in terms of stimulus reliability and probability estimation has derived from these results (Angelaki et al., 2009). In the case of flavor, psychophysical studies in humans have shown that unfamiliar odor-taste pairings are often perceived as less intense than the component stimuli, suggesting a suppressive mixture effect (Dalton et al., 2000; Gillan, 1983). In contrast, familiar taste-odor pairings (e.g. vanilla and sugar) were reported as more intense than the components and perception of novel taste-odor pairings can be altered by experience (Prescott, 2012; Small et al., 2004). Our laboratory animals are reared in a sterile, controlled environment with a reliable but monotonous diet of formulated chow. Thus, any of the taste-odor pairing provided in our experiments were novel, with the exception of flavors experienced during conditioning. Our results therefore comport with the psychophysical results seen in humans and suggest that future work could look at whether shifts in population activity are accompanied by an increased sensitivity to the mixture.

Experimental Procedures

Surgery

Surgery was performed similar to previous published insular imaging experiments with the addition of a retronasal intubation (Chen et al., 2011). Briefly, Thy1-Gcamp6s 4.12 mice were anaesthetized with urethane (1.8g/kg), delivered in two i.p. Injections separated by 20 minutes. Body temperature was maintained at 36-37 C throughout the experiment with a feedback-controlled heating pad (FHC). Animals were double-tracheotomized with one tube going to the lungs to ensure a clear airway and the other port going to the nasopharynx to permit retronasal delivery of odor stimuli. A steel headpost was mounted on the animal's skull with dental acrylic (ortho-jet) and affixed in a custom holder to permit stabilization and manipulation of the head. The skin and portions of the masseter muscle were removed and after cutting the zygomatic arch the mandible was retracted to expose the ventrolateral surface of the skull. An ~2mm craniotomy centered dorso-ventrally around the lower branch of the rhinal vein and delimited anteriorly by the middle cerebral artery was drilled with periodic breaks to wash away cuttings and cool the site using calcium free aCSF (150 mM NaCl, 2.5 mM KCl, 10 mM HEPES) (Stettler and Axel, 2009). Bone was gingerly removed using ceramic coated forceps (FST). In some animals, if the dura was compromised during removal of bone flap, the dura was retracted. The brain was covered with a fragment of #0 glass coverslip, aCSF with 2% agarose was applied at the edges of the coverslip, and it was fixed in place with vetbond and dental acrylic. A custom well was constructed from parafilm and vetbond to hold liquid for dipping objectives.

2-Photon Imaging

Calcium Imaging was carried out using a two-photon microscope with a Nikon 16x 0.8 N.A. water immersion objective. This provided an ~850 μm field of view that could be scanned at ~30hz 512x512 using a resonant scanner. In all experiments a piezo device was used to near simultaneously scan between 2-4 planes in the z-axis, typically reducing the acquision rate to between 4 and 9 Hz depending on various settings. All acquired planes were at least 30um apart to decrease signal crosstalk between planes (see also post-processing). The excitation wavelength was 920 nm and fluorescence emission was filtered with a 580 dcxr dichroic and hq525/70 m-2p bandpass filter. Taste stimuli were delivered rapidly (> 2 ml / min.) to the entire tongue and oral cavity using a pressure-controlled perfusion system. For all experiments, a 30 s pre-stimulus application of distilled water preceded a 5s exposure to the test tastants and was followed by a 30s wash; inter-trial window was approx. 2 min. Unlike studies in visual, auditory or somatosensory system where the stimuli can be delivered and removed within milliseconds, and dozens of trials readily tested, the need to deliver significant amount of fluid to the tongue, and to thoroughly remove and wash the oral cavity between trials necessitates long trial times, thus limiting the total number of trials that can be tested in any one experiment. Taste, Odor, and Mixture trials were interleaved in pseudorandomized order. Only experiments with five or more trials of a given stimulus were included in analysis. Tastants were: 10mM quinine, 30mM sucralose, 300mM sucrose. Odorants were made fresh daily and allowed to disperse for at least one hour. A constant stream of air and odor stimulations were delivered through ptfe tubing with a flow rate of 100-200ml/min using an olfactometer (aurora scientific 206a). Starting Odorant concentrations were: amy-acetate (.01% in mineral_oil), ethyl-butyrate (.01% in mineral-oil),

grape-koolaid(1% in dH2O), cherry-koolaid(1% in dH2O). All odors were diluted 1:10 with carrier air before delivery to animal. Odor pulse timing was measured with a photo-ionization detector (aurora scientific 200b mini-pid). The animal's face was recorded with an IR camera to verify the integrity of the experiments both during and post-hoc.

Image Processing and Analysis

All imaging data was recorded and processed as individual trials. Because the trials were acquired over several hours, small changes precluded the concatenation of trials and analysis as a continuous recording. For instance, evaporative loss of immersion liquid could cause a decrease in the effective numerical aperture, leading to a decrease in axial resolution and general brightening of the entire image. Movies were first separated by recorded plane and aligned using the Suite2p python package (Pachitariu et al., 2017). Movies were then imported into ImageJ where regions of interest encompassing cell somata were segmented semi-manually using the Cell Magic Wand Tool (Theo Walker). Neuropil contamination was corrected using the python package FISSA, which performed source separation (Keemink et al., 2018). The resultant delta f (calculated as F0/(F-F0) where F0 is the 5th percentile of a given trial), was denoised using the oasis denoising and deconvolution package in MATLAB (Friedrich et al., 2017). Cells were then classified according to previously published methods (Barretto et al., 2015). Briefly, each trace was converted to a modified z-score and trials which had activity exceeding 3.5 z-scores for at least 2 seconds in the stimulus window were categorized as responsive trials. If a cell responded in more than half of trials of a given stimulus, it was classified as a responder. For both PCA and calculation of Additivity Index, the range of a cells response in delta f from start of stimulus to 1s after end of stimulus was used. For PCA, a pseudovector of responses was

created with columns being cells that responded to at least one of the stimuli included in the matrix and rows being amplitudes on individual trials. Principal Components and projected data were then calculated using the Dimensionality Reduction Toolbox (https://lvdmaaten.github.io/drtoolbox). PC distances were computed according to Bolding et. al: "3-dimensional Euclidean distances were computed for each trial pair and the average trial pair distance was computed for each stimulus" (Bolding and Franks, 2018)

Flavor Conditioning

Mice were single housed in custom chambers with two bottle ports. Initial odor preference to either grape or cherry (.1% unsweetened kool-aid in distilled water) was determined with a 24-hour assay. Next, initial sweetener preference for either 300mM sucrose or 8mM sucralose was determined with a 24-hour assay. The less preferred odor was then paired with sucrose and vice-versa. These solutions were serially provided to the animal for 48-hour periods alongside a bottle of water. After four alternating exposures (8 days), mice were tested in a 24-hour post-conditioning two bottle assay with both flavor solutions. Post-conditioning odor preference was then determined in a 24-hour assay. Mice were then continuously provided with 2 flavor bottles until imaged.

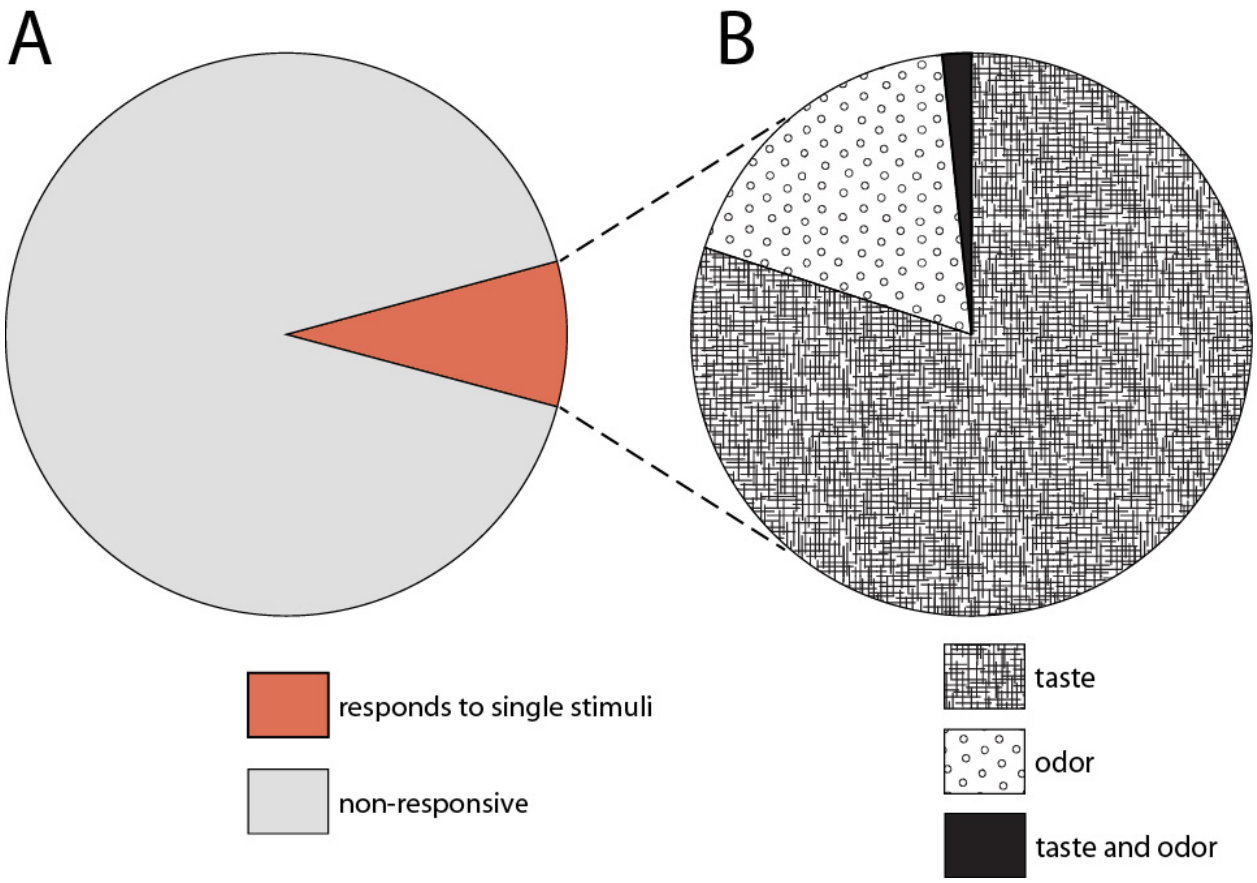

Fig 2.16: Summary of all single modality stimulus responders

A. Of the 10,508 cells recorded across 29 animals, 8% responded to at least one taste or odor. **B.** Of the responding subpopulation, approximately 80% responded to taste alone, 18% responded to odor alone, and 2% responded to odor or taste.

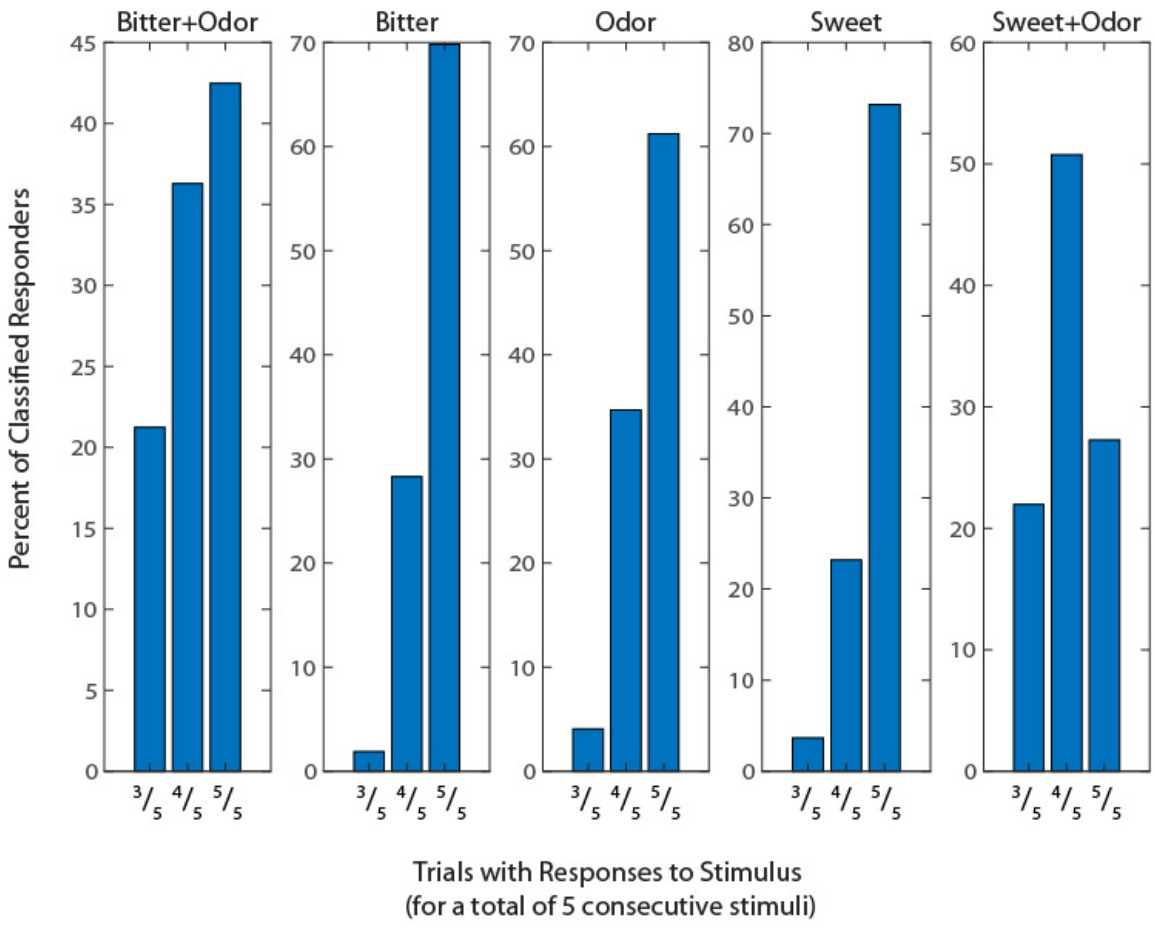

Fig 2.17 Response Reliability for Different Stimuli

The first five trials of a stimulus were analyzed and the probability that a classified responder responded in 3/5, 4/5 or 5/5 trials was calculated.

Chapter 3

Silencing Agranular Insular Cortex During a Flavor Discrimination Task

Introduction

Our understanding of perception and decision-making has benefited from the use of experiments designed to measure specific motor outputs in response to controlled stimuli (Gold and Shadlen, 2007; Panzeri et al., 2017). These psychophysical tasks were typically applied to primates, but they are increasingly used in rodents, providing insight into somatosensory, auditory, and visual perception and decision making (Carandini and Churchland, 2013). In order to test the role of AIc in odor-taste integration, we used a two-alternative forced choice design in which a water deprived animal is presented with either an odor, a taste, or a mixture at a center sampling port (Fig 3A). After sampling the test stimulus, the animal learns to report its perception by licking at a reward port to the left or right. In these experiments one side was rewarded after sampling the mixture while the other side was rewarded after sampling either of the mixture components.

Results

Animals can learn the task and perform with greater than 90% accuracy for any given stimulus (Fig 3.1). We next asked whether the animals would still be able to discriminate between stimuli when AIc was silenced. Given that AIc is a long thin parcel of cortex which could not be targeted with a single viral injection, we took several measures to increase the

likelihood of selectively silencing AIc. First, we lesioned the cortical area encompassing AIc in one hemisphere with a unilateral injection of ibotenic acid (Pai et al., 2011; Schwarcz et al., 1979). Second, we relied on separation of anatomical outputs of AIc. Specifically, AIc preferentially projects to infralimbic cortex relative to either gustatory or piriform cortex (Fig 3.2) (Zingg et al., 2014). Therefore, we injected retrograde AAV-cre into infralimbic cortex and next injected cre dependent inhibitory DREADD (designer receptor exclusively activated by designer drugs) (Fig 3.3) (Stachniak et al., 2014; Tervo et al., 2016). This allowed for selective and reversible inactivation of AIc. While these experiments are on-going, preliminary results suggest that selective activation of AIc disrupts perception of the flavor mixture causing the animal to treat it as one of the components ($n=3$, $p=0.008$, paired t-test, baseline vs. silenced mixture) (Fig 3.4,3.5).

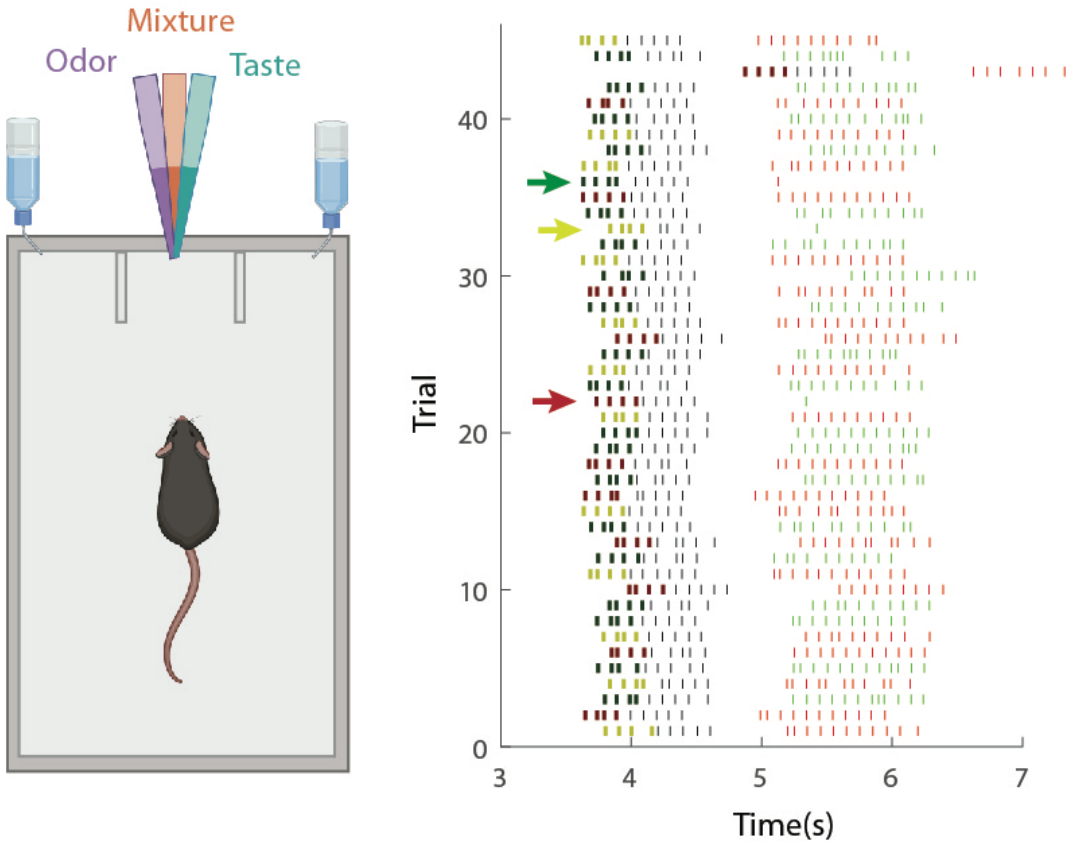

Fig 3.1: 2-AFC Flavor Discrimination Task and Typical Trial Raster

A mouse first samples several licks of the test solution at the center port. Bold colored ticks in raster indicate test solution valve opening, subsequent grey licks are dry licks prior to shutter closing. The mouse then reports it's perception by licking at one of the reward spouts. Repeated colored ticks after ~5s mark are successful trials, single colored ticks are error trials. Bold colored arrows show error trials colored by the test stimulus (red=sucralose, yellow=amyl-acetate, green=mixture).

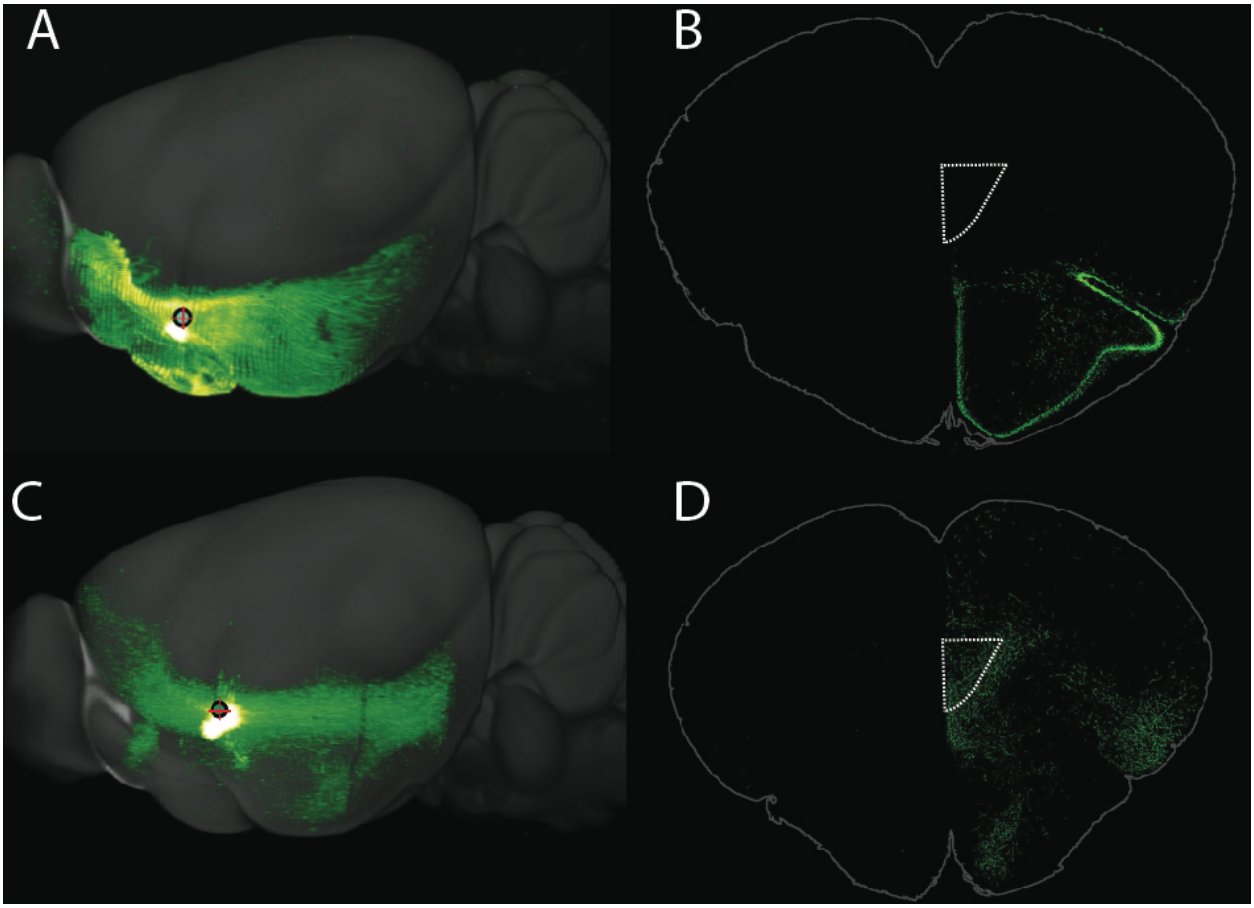

Fig 3.2: Agranular Cortex Preferentially Projects to Infralimbic Cortex

A. Viral tracing originating in Piriform cortex shows reconstruction of terminals from serial sections covering olfactory cortical regions. Circle represents the site of injection. **B**. Projections from Piriform are absent in Infralimbic Cortex (dotted white line). **C**. As in A, injection originating in Agranular Insular Cortex. **D**. AIc projection terminals can be seen in Infralimbic Cortex. (Allen Institute).

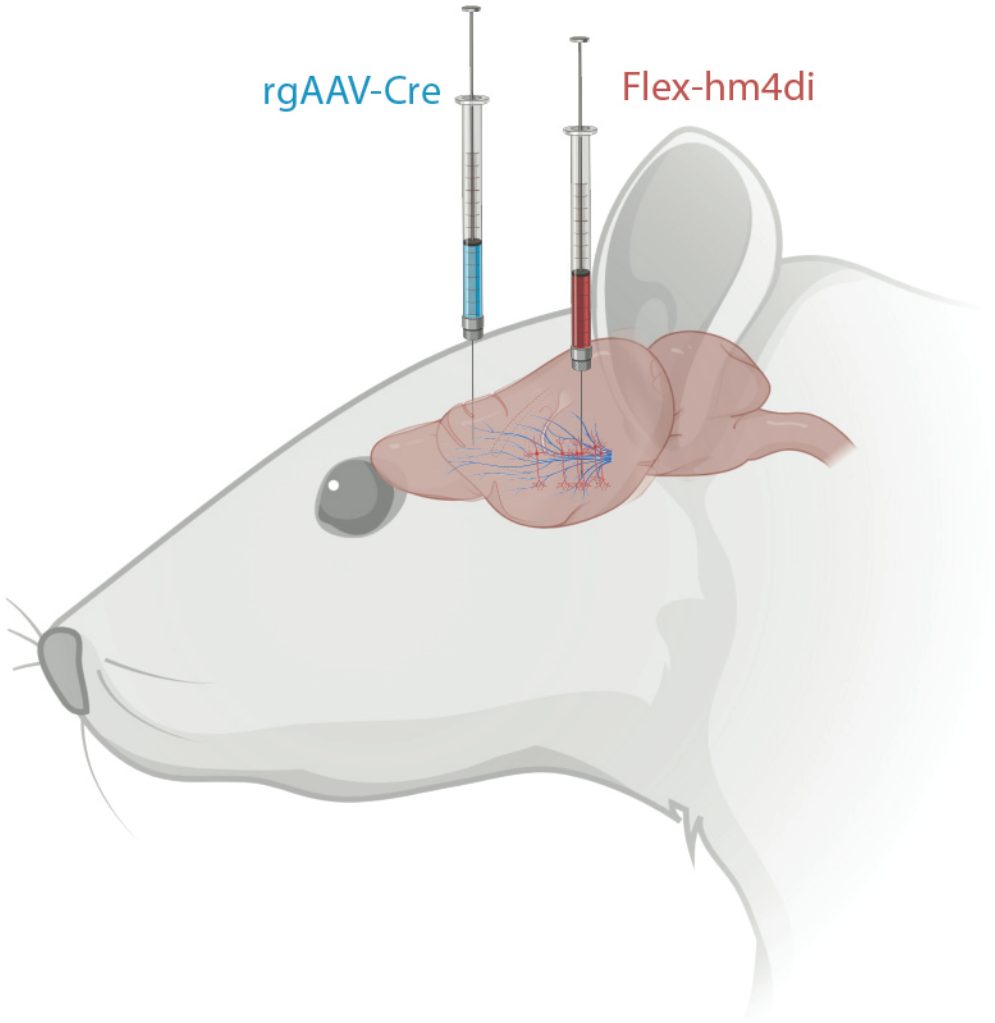

Fig 3.3: Reductionist Silencing Strategy

Animals were simultaneously injected with retrograde-AAV-Cre in infralimbic cortex and cre-dependent inhibitory DREADD targeted to AIc.

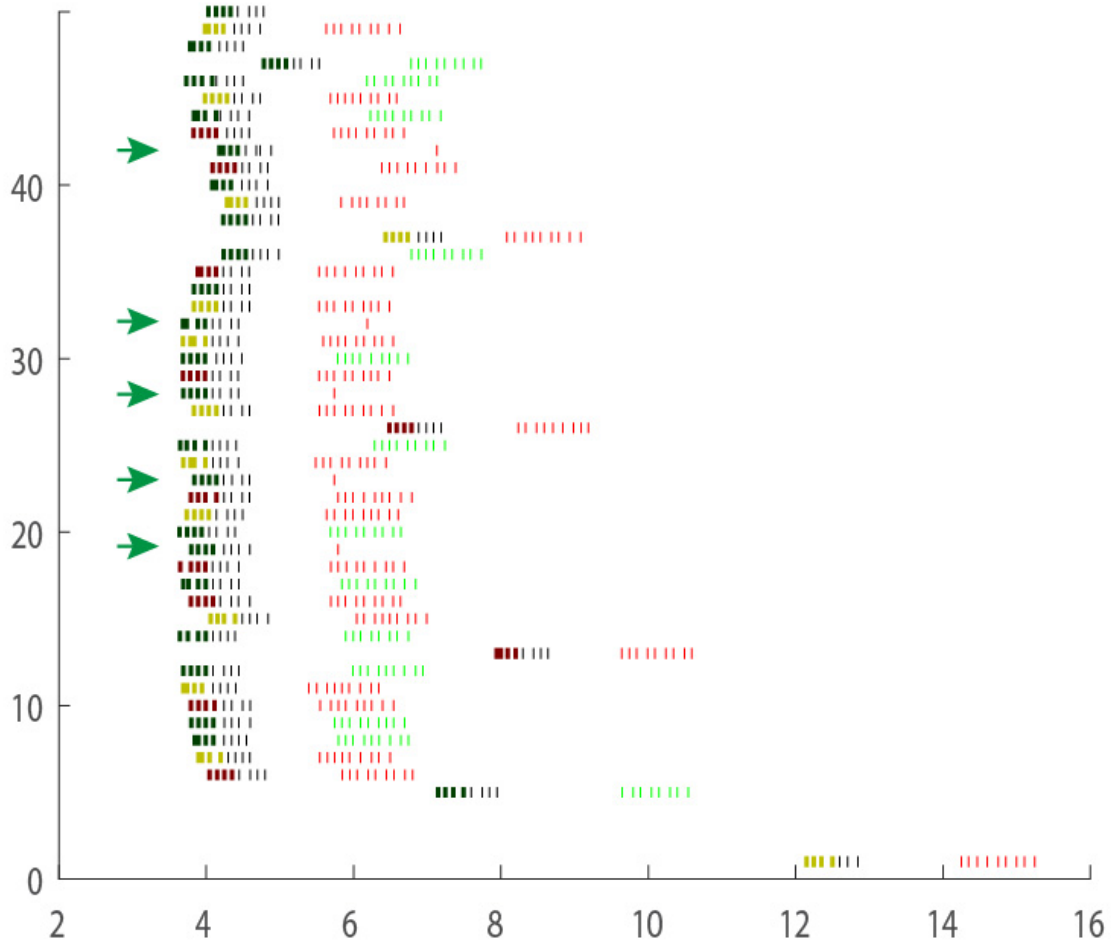

Fig 3.4: Example Raster During Alc Silenced Trials

After silencing with DREADD agonist, the animal shows selective deficits on mixture trials. For raster interpretation see explanation in Fig 3.1. Arrows point to error trials, which all occurred in response to mixture.

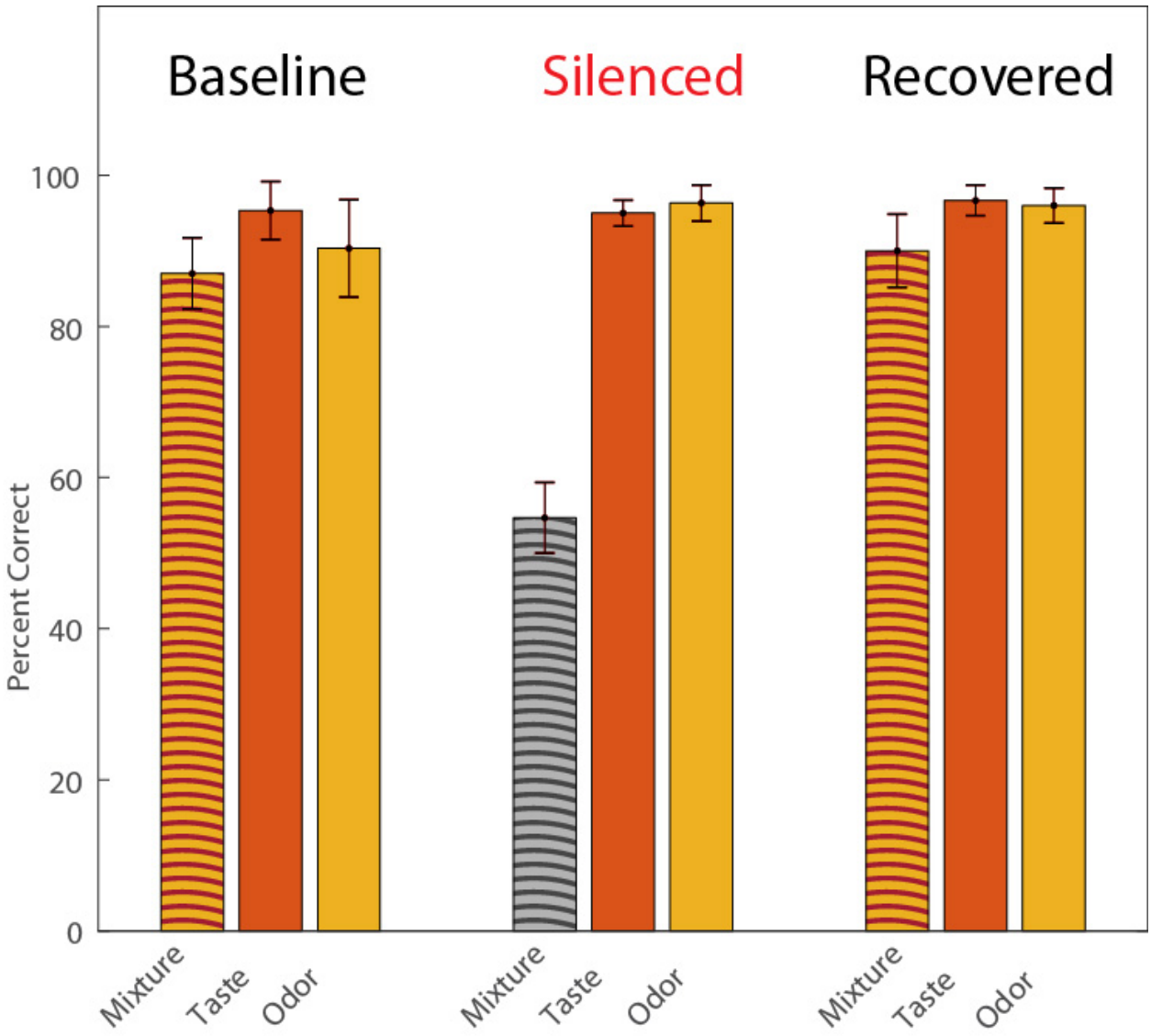

Fig 3.5: Summary of Silencing AIc

Animals learn to distinguish a mixture from its component stimuli, responding with ~90% accuracy to all categories (Baseline). Silencing of AIc selectively impairs responses to the mixture (Silenced). This deficit in flavor perception is temporary and animals show complete recovery of performance when tested after 24 hours (n=3 mice).

Discussion

Imaging agranular insula cortex showed that responses to mixtures are distinct from the component stimuli. To determine whether this mixture information was being used to drive behavior, we used a perceptual discrimination task and transient inactivation of AIc. These experiments show that flavor responses seen in AIc are read out to drive behavioral discrimination.

Perturbation of a single region could still have distal effects in a dynamical system such as the brain, potentially affecting the ability of downstream regions to perform computations or instantiate motor actions that are required to complete the task. In our silencing, we have the component stimuli as a control, demonstrating that the silencing does not perturb systems that are required to perform the task. In earlier iterations of our experiments, misplaced injections of DREADDs into olfactory or gustatory regions occasionally caused deficits in unisensory responses while not affecting responses to the mixture (data not shown). This suggests that a weakened unisensory input can be detected by AIc, possibly through experience dependent enhancement (these animals have thousands of trials of experience with the mixture by the time of inactivation experiments).

What does an animal that is simultaneously experiencing taste and odor but not the mixture perceive? Sensory selection studies have looked at how animals selectively attend to one modality when presented with a multimodal stimulus (Wimmer et al., 2015). (Wimmer et al., 2015). This sensory selection is a learned contextual task switching behavior that seems to be controlled by anticipatory biasing of sensory input through prefontal modulation of thalamic input. In our behavior, the odor and taste would presumably be experienced simultaneously but

there is no contextual dependency and the behavioral response to either input alone is the same (since both are rewarded at the same response port). One option to dismabiguate the perceived stimulus would be to separate odor and taste responses by using an additional reward port. This would increase the complexity of a task which already takes several weeks to learn. Additionally, if the animals only experienced the AIc silenced mixture as odor or taste, we would expect it to respond incorrectly 100% of the time. One way to interpret the decision making would be to record from downstream neurons that are accumulating evidence and look for differences in activity that are unique to the three stimuli categories and compare that to silenced trial mixture responses.

Experimental Procedures

Viral Injections

Animals were injected as described in Chapter 1. Mice were injected unilaterally with 300nL of ibotenic acid (10mg/mL) at 4 locations (0.0 AP, 3.8ML, 3.3Z), (0.0 AP, 3.8ML, 2.5Z), (+1.3 AP, 3.5 ML, 2.8 Z), (+1.3 AP, 3.5 ML, 2.1 Z). For infralimbic cortical injections, 100nL of AAVrg-pmSyn1-EBFP-Cre was injected contralaterally to the ibotenic acid injection at (+1.8 AP, 0.3 ML, 2.4Z). For Agranular Insula injetions, 100nL of AAV5-hSyn-DIO-hM4D(Gi)-mCherry was injected at two locations: (0.0 AP, 3.8mL, 3.0Z) and (+1.3 AP, 3.5 ML, 2.8 Z).

Mouse Behavior

Mice deprived of water for 24 h were trained to perform a taste-recognition task in a customized three-port behavior chamber in which they sampled taste (1mM sucralose) , odor (0.05% amyl-acetate), or mixture (0.05% amyl acetate in 1mM sucralose) stimuli from the middle port and then reported the identity of the cue by choosing to lick from either the left or right port. Cues were pseudo-randomly delivered through a metal spout in the middle port. Each trial began with the shutter opening in the middle port. Mice were given (up to) 20 s to initiate a trial by licking the middle spout (failure to initiate a trial resulted in the shutter closing and a new trial starting after ~5s of tubing washout). The shutter in the middle port closed 0.5 s after the fourth lick (~3 ul); 0.5 s after the middle port closed, the shutters of the left and right ports opened simultaneously. Mice were given 5 s to make a left or right choice and obtain 1 s of water reward (total ~8 μl). For a given mouse, reward from side ports was assigned to either mixture cues or mixture component cues (for example, left for sweet or odor, right for sweet+odor). The inter-

trial interval was the time of washout. Mice were trained for two sessions per day, with 50–80 pseudo-randomized trials per session until they could effectively discriminate the tastants with approximately 90% accuracy (2–3 weeks). To test the effect of silencing Agranular Insula, mice were injected with 1mg/kg of the hm4di agonist Olazapine at a concentration of .2mg/mL. Performances were calculated as the percentage of correct choices for a given taste cue. The lick behavior was detected by a capacitive touch sensor (MPR121, SparkFun). The delivery of tastants, shutter position and light stimuli were controlled by a custom-written program in MATLAB via an Arduino board.

Conclusions

Our experience of the world is formed from disparate sensory systems which collect a piecemeal survey of the environment. Where and how different senses come together is an ongoing focus of research. Here we focused on the multisensory concept of flavor which is primarily comprised of taste and smell, two senses with unique but complementary purposes. We now know understand the anatomy and physiology of gustation and olfaction, yet there is little understanding of where these chemical senses combine to form perception of flavor.

This thesis demonstrates first that these senses, which necessarily are close enough at the periphery to detect chemicals originating from the same substance and yet send segregated streams of information to the brain, eventually converge in agranular insular cortex. We then used *in vivo* calcium imaging to characterize responses to taste and odor in AIc, showing that while representations of different taste qualities are interdigitated in non-overlapping populations, odor representations have a greater degree of overlap. To our knowledge, no research has been performed looking at how the combination of these sense is represented in the individual cells' neural responses. We found that flavor mixtures activated a unique population consisting of some cells that responded to taste and/or odor as well as cells that only responded to the mixture. This multisensory representation differed from either of the unisensory populations with some mixture responsive cells showing enhancement and some showing suppression. Human psychophysical studies of flavor have reported that experience of a taste-odor mixture increases the perceived intensity of that flavor but the mechanisms behind this plasticity are unknown. We found that repeated exposure to a flavor caused an increase in mixture responsive cells and shifted the distribution of additivity indices towards enhancement. Finally, we developed a two-alternative forced choice behavior paradigm to test whether AIc

plays a causal role in an animal's behavioral response to a perceived flavor. We find that silencing AIc selectively impairs the ability to correctly respond to a taste-odor mixture while not affecting performance in response to taste or odor alone. Taken together, these results provide a substantial body of evidence that agranular insular cortex is the site of taste-odor integration in the mouse brain.

References

Accolla, R., Bathellier, B., Petersen, C.C.H., and Carleton, A. (2007). Differential Spatial Representation of Taste Modalities in the Rat Gustatory Cortex. J. Neurosci. *27*, 1396–1404.

Adler, E., Hoon, M.A., Mueller, K.L., Chandrashekar, J., Ryba, N.J.P., and Zuker, C.S. (2000). A Novel Family of Mammalian Taste Receptors. Cell *100*, 693–702.

Angelaki, D.E., Gu, Y., and DeAngelis, G.C. (2009). Multisensory integration. Curr Opin Neurobiol *19*, 452–458.

Barretto, R.P.J., Gillis-Smith, S., Chandrashekar, J., Yarmolinsky, D.A., Schnitzer, M.J., Ryba, N.J.P., and Zuker, C.S. (2015). The neural representation of taste quality at the periphery. Nature *517*, 373–376.

Bolding, K.A., and Franks, K.M. (2018). Recurrent cortical circuits implement concentration-invariant odor coding. BioRxiv.

Buck, L., and Axel, R. (1991). A novel multigene family may encode odorant receptors: A molecular basis for odor recognition. Cell *65*, 175–187.

Bushdid, C., Magnasco, M.O., Vosshall, L.B., and Keller, A. (2014). Humans Can Discriminate More than 1 Trillion Olfactory Stimuli. Science *343*, 1370–1372.

Carandini, M., and Churchland, A.K. (2013). Probing perceptual decisions in rodents. Nat Neurosci *16*, 824–831.

Chandrashekar, J., Mueller, K.L., Hoon, M.A., Adler, E., Feng, L., Guo, W., Zuker, C.S., and Ryba, N.J.P. (2000). T2Rs Function as Bitter Taste Receptors. Cell *100*, 703–711.

Chen, X., Gabitto, M., Peng, Y., Ryba, N.J.P., and Zuker, C.S. (2011). A Gustotopic Map of Taste Qualities in the Mammalian Brain. Science *333*, 1262–1266.

Chet, I., Naveh, A., and Henis, Y. (1977). Chemotaxis of Physarum polycephalum towards Carbohydrates, Amino Acids and Nucleotides. Journal of General Microbiology *102*, 145–148.

Choi, G.B., Stettler, D.D., Kallman, B.R., Bhaskar, S.T., Fleischmann, A., and Axel, R. (2011). Driving Opposing Behaviors with Ensembles of Piriform Neurons. Cell *146*, 1004–1015.

Dalton, P., Doolittle, N., Nagata, H., and Breslin, P. a. S. (2000). The merging of the senses: integration of subthreshold taste and smell. Nature Neuroscience *3*, 431.

Damak, S. (2003). Detection of Sweet and Umami Taste in the Absence of Taste Receptor T1r3. Science *301*, 850–853.

Desgranges, B., Ramirez-Amaya, V., Ricaño-Cornejo, I., Lévy, F., and Ferreira, G. (2010). Flavor Preference Learning Increases Olfactory and Gustatory Convergence onto Single Neurons in the Basolateral Amygdala but Not in the Insular Cortex in Rats. PLOS ONE *5*, e10097.

Ercsey-Ravasz, M., Markov, N.T., Lamy, C., Van Essen, D.C., Knoblauch, K., Toroczkai, Z., and Kennedy, H. (2013). A Predictive Network Model of Cerebral Cortical Connectivity Based on a Distance Rule. Neuron *80*, 184–197.

Friedrich, J., Zhou, P., and Paninski, L. (2017). Fast online deconvolution of calcium imaging data. PLOS Computational Biology *13*, e1005423.

Furudono, Y., Cruz, G., and Lowe, G. (2013). Glomerular input patterns in the mouse olfactory bulb evoked by retronasal odor stimuli. BMC Neurosci *14*, 45.

Ghazanfar, A.A., and Schroeder, C.E. (2006). Is neocortex essentially multisensory? Trends in Cognitive Sciences *10*, 278–285.

Ghosh, S., Larson, S.D., Hefzi, H., Marnoy, Z., Cutforth, T., Dokka, K., and Baldwin, K.K. (2011). Sensory maps in the olfactory cortex defined by long-range viral tracing of single neurons. Nature *472*, 217–220.

Giessel, A.J., and Datta, S.R. (2014). Olfactory Maps, Circuits and Computations. Curr Opin Neurobiol *0*, 120–132.

Gillan, D.J. (1983). Taste-taste, odor-odor, and taste-odor mixtures: Greater suppression within than between modalities. Perception & Psychophysics *33*, 183–185.

Godfrey, P.A., Malnic, B., and Buck, L.B. (2004). The mouse olfactory receptor gene family. Proceedings of the National Academy of Sciences *101*, 2156–2161.

Gogolla, N. (2017). The insular cortex. Current Biology *27*, R580–R586.

Gold, J.I., and Shadlen, M.N. (2007). The Neural Basis of Decision Making. Annual Review of Neuroscience *30*, 535–574.

Gore, F., Schwartz, E.C., Brangers, B.C., Aladi, S., Stujenske, J.M., Likhtik, E., Russo, M.J., Gordon, J.A., Salzman, C.D., and Axel, R. (2015). Neural Representations of Unconditioned Stimuli in Basolateral Amygdala Mediate Innate and Learned Responses. Cell *162*, 134–145.

Gradinaru, V., Zhang, F., Ramakrishnan, C., Mattis, J., Prakash, R., Diester, I., Goshen, I., Thompson, K.R., and Deisseroth, K. (2010). Molecular and Cellular Approaches for Diversifying and Extending Optogenetics. Cell *141*, 154–165.

Grill, H.J., and Norgren, R. (1978). The taste reactivity test. II. Mimetic responses to gustatory stimuli in chronic thalamic and chronic decerebrate rats. Brain Research *143*, 281–297.

Hooks, B.M., Lin, J.Y., Guo, C., and Svoboda, K. (2015). Dual-Channel Circuit Mapping Reveals Sensorimotor Convergence in the Primary Motor Cortex. J. Neurosci. *35*, 4418–4426.

Johnson, D.M.G., Illig, K.R., Behan, M., and Haberly, L.B. (2000a). New Features of Connectivity in Piriform Cortex Visualized by Intracellular Injection of Pyramidal Cells Suggest that “Primary” Olfactory Cortex Functions Like “Association” Cortex in Other Sensory Systems. The Journal of Neuroscience *20*, 6974–6982.

Johnson, D.M.G., Illig, K.R., Behan, M., and Haberly, L.B. (2000b). New Features of Connectivity in Piriform Cortex Visualized by Intracellular Injection of Pyramidal Cells Suggest that “Primary” Olfactory Cortex Functions Like “Association” Cortex in Other Sensory Systems. The Journal of Neuroscience *20*, 6974–6982.

Keemink, S.W., Lowe, S.C., Pakan, J.M.P., Dylda, E., van Rossum, M.C.W., and Rochefort, N.L. (2018). FISSA: A neuropil decontamination toolbox for calcium imaging signals. Sci Rep *8*, 3493.

Lee, H., Macpherson, L.J., Parada, C.A., Zuker, C.S., and Ryba, N.J.P. (2017). Rewiring the taste system. Nature *548*, 330–333.

Libbrecht, S., Van den Haute, C., Malinouskaya, L., Gijsbers, R., and Baekelandt, V. (2017). Evaluation of WGA–Cre-dependent topological transgene expression in the rodent brain. Brain Struct Funct *222*, 717–733.

Lindemann, B. (2001). Receptors and transduction in taste. Nature *413*, 219.

Llinás, R.R. (2003). The contribution of Santiago Ramon y Cajal to functional neuroscience. Nature Reviews Neuroscience *4*, 77.

Maier, J.X., Wachowiak, M., and Katz, D.B. (2012). Chemosensory Convergence on Primary Olfactory Cortex. J. Neurosci. *32*, 17037–17047.

Matsunami, H., Montmayeur, J.-P., and Buck, L.B. (2000). A family of candidate taste receptors in human and mouse. *404*, 4.

Meister, M. (2015). On the dimensionality of odor space. ELife *4*.

Mori, K., and Yoshihara, Y. (1995). Molecular recognition and olfactory processing in the mammalian olfactory system. Progress in Neurobiology *45*, 585–619.

Mueller, K.L., Hoon, M.A., Erlenbach, I., Chandrashekar, J., Zuker, C.S., and Ryba, N.J.P. (2005). The receptors and coding logic for bitter taste. Nature *434*, 225–229.

Nelson, G., Hoon, M.A., Chandrashekar, J., Zhang, Y., Ryba, N.J.P., and Zuker, C.S. (2001). Mammalian Sweet Taste Receptors. Cell *106*, 381–390.

Norgren, R., and Leonard, C.M. (1973). Ascending central gustatory pathways. Journal of Comparative Neurology *150*, 217–237.

Oh, S.W., Harris, J.A., Ng, L., Winslow, B., Cain, N., Mihalas, S., Wang, Q., Lau, C., Kuan, L., Henry, A.M., et al. (2014). A mesoscale connectome of the mouse brain. Nature *508*, 207–214.

Ongur, D. (2000). The Organization of Networks within the Orbital and Medial Prefrontal Cortex of Rats, Monkeys and Humans. Cerebral Cortex *10*, 206–219.

Pachitariu, M., Stringer, C., Dipoppa, M., Schröder, S., Rossi, L.F., Dalgleish, H., Carandini, M., and Harris, K.D. (2017). Suite2p: beyond 10,000 neurons with standard two-photon microscopy. BioRxiv.

Pai, S.S., Erlich, J.C., Kopec, C., and Brody, C.D. (2011). Minimal Impairment in a Rat Model of Duration Discrimination Following Excitotoxic Lesions of Primary Auditory and Prefrontal Cortices. Front. Syst. Neurosci. *5*.

Panzeri, S., Harvey, C.D., Piasini, E., Latham, P.E., and Fellin, T. (2017). Cracking the Neural Code for Sensory Perception by Combining Statistics, Intervention, and Behavior. Neuron *93*, 491–507.

Peng, Y., Gillis-Smith, S., Jin, H., Tränkner, D., Ryba, N.J.P., and Zuker, C.S. (2015). Sweet and bitter taste in the brain of awake behaving animals. Nature *527*, 512–515.

Perin, R., Berger, T.K., and Markram, H. (2011). A synaptic organizing principle for cortical neuronal groups. PNAS *108*, 5419–5424.

Prescott, J. (2012). Chemosensory learning and flavour: Perception, preference and intake. Physiology & Behavior *107*, 553–559.

Roland, B., Deneux, T., Franks, K.M., Bathellier, B., and Fleischmann, A. (2017). Odor identity coding by distributed ensembles of neurons in the mouse olfactory cortex. ELife *6*, e26337.

Rolls, E., and Baylis, L. (1994). Gustatory, olfactory, and visual convergence within the primate orbitofrontal cortex. The Journal of Neuroscience *14*, 5437–5452.

Root, C.M., Denny, C.A., Hen, R., and Axel, R. (2014). The participation of cortical amygdala in innate, odour-driven behaviour. Nature *515*, 269–273.

Samuelsen, C.L., and Fontanini, A. (2017). Processing of Intraoral Olfactory and Gustatory Signals in the Gustatory Cortex of Awake Rats. J. Neurosci. *37*, 244–257.

Saper, C.B., and Loewy, A.D. (1980). Efferent connections of the parabrachial nucleus in the rat. Brain Research *197*, 291–317.

Schroeder, C.E., Smiley, J., Fu, K.G., McGinnis, T., O'Connell, M.N., and Hackett, T.A. (2003). Anatomical mechanisms and functional implications of multisensory convergence in early cortical processing. International Journal of Psychophysiology *50*, 5–17.

Schwarcz, R., H□kfelt, T., Fuxe, K., Jonsson, G., Goldstein, M., and Terenius, L. (1979). Ibotenic acid-induced neuronal degeneration: A morphological and neurochemical study. Experimental Brain Research *37*.

Sclafani, A., Glass, D.S., Margolskee, R.F., and Glendinning, J.I. (2010). Gut T1R3 sweet taste receptors do not mediate sucrose-conditioned flavor preferences in mice. Am. J. Physiol. Regul. Integr. Comp. Physiol. *299*, R1643-1650.

Scott, T.R., and Small, D.M. (2009). The role of the parabrachial nucleus in taste processing and feeding. Ann. N. Y. Acad. Sci. *1170*, 372–377.

Sewards, T.V., and Sewards, M.A. (2001). Cortical association areas in the gustatory system. Neuroscience & Biobehavioral Reviews *25*, 395–407.

Shepherd, G.M. (2005). Perception without a Thalamus: How Does Olfaction Do It? Neuron *46*, 166–168.

Shi, C.-J., and Cassell, M.D. (1998a). Cortical, thalamic, and amygdaloid connections of the anterior and posterior insular cortices. Journal of Comparative Neurology *399*, 440–468.

Shi, C.-J., and Cassell, M.D. (1998b). Cortical, thalamic, and amygdaloid connections of the anterior and posterior insular cortices. Journal of Comparative Neurology *399*, 440–468.

Shipley, M.T., and Geinisman, Y. (1984). Anatomical evidence for convergence of olfactory, gustatory, and visceral afferent pathways in mouse cerebral cortex. Brain Research Bulletin *12*, 221–226.

Small, D.M. (2012). Flavor is in the brain. Physiol. Behav. *107*, 540–552.

Small, D.M., Voss, J., Mak, Y.E., Simmons, K.B., Parrish, T., and Gitelman, D. (2004). Experience-Dependent Neural Integration of Taste and Smell in the Human Brain. Journal of Neurophysiology *92*, 1892–1903.

Sosulski, D.L., Bloom, M.L., Cutforth, T., Axel, R., and Datta, S.R. (2011). Distinct representations of olfactory information in different cortical centres. Nature *472*, 213–216.

Stachniak, T.J., Ghosh, A., and Sternson, S.M. (2014). Chemogenetic synaptic silencing of neural circuits localizes a hypothalamus→midbrain pathway for feeding behavior. Neuron *82*, 797–808.

Stein, B.E., and Stanford, T.R. (2008). Multisensory integration: current issues from the perspective of the single neuron. Nature Reviews Neuroscience *9*, 255–266.

Stein, B.E., Stanford, T.R., and Rowland, B.A. (2014). Development of multisensory integration from the perspective of the individual neuron. Nature Reviews Neuroscience *15*, 520–535.

Steiner, J.E. (1973). The gustofacial response: observation on normal and anencephalic newborn infants. Symp Oral Sens Percept 254–278.

Stettler, D.D., and Axel, R. (2009). Representations of Odor in the Piriform Cortex. Neuron *63*, 854–864.

Tervo, D.G.R., Hwang, B.-Y., Viswanathan, S., Gaj, T., Lavzin, M., Ritola, K.D., Lindo, S., Michael, S., Kuleshova, E., Ojala, D., et al. (2016). A Designer AAV Variant Permits Efficient Retrograde Access to Projection Neurons. Neuron *92*, 372–382.

Touzani, K., and Sclafani, A. (2007). Insular cortex lesions fail to block flavor and taste preference learning in rats. Eur. J. Neurosci. *26*, 1692–1700.

Wall, N.R., Wickersham, I.R., Cetin, A., Parra, M.D.L., and Callaway, E.M. (2010). Monosynaptic circuit tracing in vivo through Cre-dependent targeting and complementation of modified rabies virus. PNAS *107*, 21848–21853.

Wallace, M.T., Ramachandran, R., and Stein, B.E. (2004). A revised view of sensory cortical parcellation. Proceedings of the National Academy of Sciences *101*, 2167–2172.

Wang, L., Gillis-Smith, S., Peng, Y., Zhang, J., Chen, X., Salzman, C.D., Ryba, N.J.P., and Zuker, C.S. (2018). The coding of valence and identity in the mammalian taste system. Nature *558*, 127–131.

Wickersham, I.R., Lyon, D.C., Barnard, R.J.O., Mori, T., Finke, S., Conzelmann, K.-K., Young, J.A.T., and Callaway, E.M. (2007). Monosynaptic Restriction of Transsynaptic Tracing from Single, Genetically Targeted Neurons. Neuron *53*, 639–647.

Wimmer, R.D., Schmitt, L.I., Davidson, T.J., Nakajima, M., Deisseroth, K., and Halassa, M.M. (2015). Thalamic control of sensory selection in divided attention. Nature *526*, 705–709.

Yamamoto, T. (1984). Taste responses of cortical neurons. Progress in Neurobiology *23*, 273–315.

Yarmolinsky, D.A., Zuker, C.S., and Ryba, N.J.P. (2009). Common Sense about Taste: From Mammals to Insects. Cell *139*, 234–244.

Yizhar, O., Fenno, L.E., Prigge, M., Schneider, F., Davidson, T.J., O'Shea, D.J., Sohal, V.S., Goshen, I., Finkelstein, J., Paz, J.T., et al. (2011). Neocortical excitation/inhibition balance in information processing and social dysfunction. Nature *477*, 171–178.

Zhang, X., and Firestein, S. (2002). The olfactory receptor gene superfamily of the mouse. Nature Neuroscience *5*, 124.

Zhang, Y., Hoon, M.A., Chandrashekar, J., Mueller, K.L., Cook, B., Wu, D., Zuker, C.S., and Ryba, N.J.P. Coding of Sweet, Bitter, and Umami Tastes: Different Receptor Cells Sharing Similar Signaling Pathways. 9.

Zhao, G.Q., Zhang, Y., Hoon, M.A., Chandrashekar, J., Erlenbach, I., Ryba, N.J.P., and Zuker, C.S. (2003). The Receptors for Mammalian Sweet and Umami Taste. Cell *115*, 255–266.

Zingg, B., Hintiryan, H., Gou, L., Song, M.Y., Bay, M., Bienkowski, M.S., Foster, N.N., Yamashita, S., Bowman, I., Toga, A.W., et al. (2014). Neural Networks of the Mouse Neocortex. Cell *156*, 1096–1111.